Journal of Medicinal Chemistry

Article

pubs.acs.org/jmc

Hepatitis C Virus NS5A Replication Complex Inhibitors: The Discovery of Daclatasvir

Makonen Belema,*[,†] Van N. Nguyen,[†] Carol Bachand,[⊥] Dan H. Deon,[⊥] Jason T. Goodrich,[†] Clint A. James,[⊥] Rico Lavoie,[⊥] Omar D. Lopez,[†] Alain Martel,[⊥] Jeffrey L. Romine,[†] Edward H. Ruediger,[⊥] Lawrence B. Snyder,[†] Denis R. St. Laurent,[†] Fukang Yang,[†] Juliang Zhu,[‡] Henry S. Wong,[‡] David R. Langley,[§] Stephen P. Adams,[¶] Glenn H. Cantor,[∥] Anjaneya Chimalakonda,[∥] Aberra Fura,[△] Benjamin M. Johnson,[¶] Jay O. Knipe,[¶] Dawn D. Parker,[¶] Kenneth S. Santone,[¶] Robert A. Fridell,[#] Julie A. Lemm,[#] Donald R. O'Boyle, II,[#] Richard J. Colonno,[#] Min Gao,[#] Nicholas A. Meanwell,[†] and Lawrence G. Hamann[†]

[†]Departments of Discovery Chemistry, [‡]Discovery Chemistry Synthesis, [§]Computer-Assisted Drug Design, and [¶]Pharmaceutical Candidate Optimization, [#]Virology, Bristol-Myers Squibb Research and Development, 5 Research Parkway, Wallingford, Connecticut 06492, United States

[⊥]Department of Discovery Chemistry, Bristol-Myers Squibb Pharmaceutical Research Institute, 100 boul. De l'Industrie, Candiac, Que., Canada J5R 1J1

[∥]Department of Pharmaceutical Candidate Optimization, Bristol-Myers Squibb Research and Development, 311 Pennington-Rocky Hill Road, Pennington, New Jersey 08534, United States

[△]Department of Pharmaceutical Candidate Optimization, Bristol-Myers Squibb Research and Development, Route 206 and Province Line Road, Princeton, New Jersey 08543, United States

ABSTRACT: The biphenyl derivatives **2** and **3** are prototypes of a novel class of NS5A replication complex inhibitors that demonstrate high inhibitory potency toward a panel of clinically relevant HCV strains encompassing genotypes 1−6. However, these compounds exhibit poor systemic exposure in rat pharmacokinetic studies after oral dosing. The structure−activity relationship investigations that improved the exposure properties of the parent *bis*-phenylimidazole chemotype, culminating in the identification of the highly potent NS5A replication complex inhibitor daclatasvir (**33**) are described. An element critical to success was the realization that the arylglycine cap of **2** could be replaced with an alkylglycine derivative and still maintain the high inhibitory potency of the series if accompanied with a stereoinversion, a finding that enabled a rapid optimization of exposure properties. Compound **33** had EC_{50} values of 50 and 9 pM toward genotype-1a and -1b replicons, respectively, and oral bioavailabilities of 38−108% in preclinical species. Compound **33** provided clinical proof-of-concept for the NS5A replication complex inhibitor class, and regulatory approval to market it with the NS3/4A protease inhibitor asunaprevir for the treatment of HCV genotype-1b infection has recently been sought in Japan.

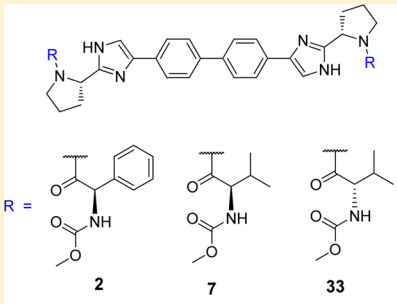

Compd	EC_{50} (nM) GT-1a	GT-1b
2	0.028	0.0067
7	1240	1.22
33	0.050	0.009

INTRODUCTION

The current optimal therapy for the treatment of hepatitis C virus (HCV) genotype-1 (GT-1) infection, the most prevalent strain, is a combination of pegylated interferon-α and the nucleoside analogue ribavirin in conjunction with either the nonstructural 3/4A (NS3/4A) protease inhibitor simeprevir or the NS5B nucleotide polymerase inhibitor sofosbuvir.[1] Although this drug regimen improves response rates compared to therapy with pegylated interferon-α and ribavirin alone, it is difficult to tolerate because of numerous side effects, some of which present a significant challenge. As part of the effort to identify direct-acting antiviral agents (DAAs) that exhibit improved efficacy and tolerability, considerable emphasis has been focused on inhibitors of the NS3/4A protease and the NS5B polymerase because these enzymes are readily recapitulated in biochemical assays that facilitate screening and evaluation of lead candidates. However, the clinical validation of NS5A replication complex inhibitors by daclatasvir (**33**) generated significant interest in this target class, as reflected by the increased number of NS5A-targeting compounds currently undergoing clinical evaluation.[2,3] Although HCV NS5A is not associated with any enzymatic

Special Issue: HCV Therapies

Received: November 27, 2013
Published: February 12, 2014

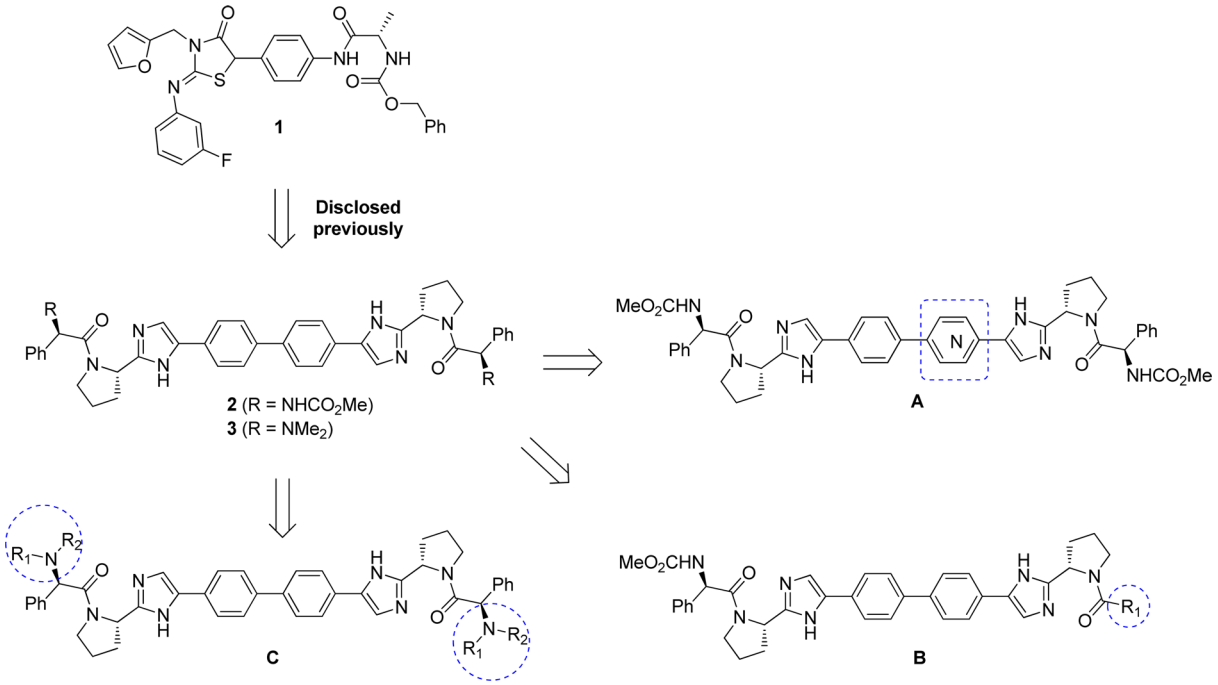

Figure 1. Initial strategies pursued to enhance PK properties of **2** and **3**.

Table 1. Replicon and Pharmacokinetic Assessment of Aza-Core Analogues 4–6[a]

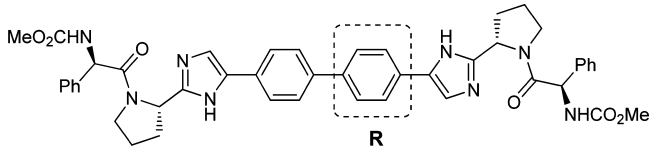

Compd	R	EC_{50} (nM) GT-1a GT-1b	EC_{50} (nM) BVDV	Solubility[b] (mg/mL)	PAMPA[b] (nm/s)	Rat PK studies[c] IV (2 mg/kg); PO (5 mg/kg)
2[d]		0.028 0.0067	1460	0.001	Null[e]	4 h PO screen (n = 2) AUC: NC Liver-4 h: ND Plasma-4 h: ND
4		0.76 0.02	4340	0.003	177	
5		3.1 0.017	3780	0.002	179	
6		1.43 0.036	4840	0.007	186	24 h IV/PO study (n = 3) IV: CL (36 mL/min·kg); Vd (1.7 L/kg); $t_{1/2}$ (1.7 h) PO: AUC (21 nM·hr); liver-24 h & plasma-24 h (ND); F (0.5%)

[a]GT-1b CC_{50} >10 μM. [b]Amorphous solubility and PAMPA values were determined at pH 6.5 and pH 7.4, respectively. [c]NC = not calculated; ND = not detected. [d]Reported previously in ref 6f. [e]Null = compound was not detected by UV plate reader in both the receiver and donor assay wells.

activity, various studies indicate that this protein plays diverse but not well-defined functions in the replication cycle of the virus.

Leads that disrupt the function of the NS5A replication complex were discovered using a phenotypic screen based on a GT-1b replicon system.[4,5] We have recently disclosed the key milestones that marked the evolution of our HCV NS5A replication complex inhibitor program, beginning from the identification of thiazolidinone **1** as a screen hit to the elucidation of a novel and potent *bis*-phenylimidazole chemotype.[4b,c,6] Notable issues that were addressed in this process included chemical instability, a potential genotoxic liability, and initial antiviral activity of limited scope toward HCV genotypes. While the picomolar inhibitory activity of the *bis*-phenylimidazole series accomplished with two related analogues, carbamate **2** and amine **3**, toward a broad panel of replicon strains was attractive, their pharmacokinetic (PK) evaluation in rats revealed poor systemic exposure following oral dosing.[6f] Thus, improving the PK properties of this series while retaining the antiviral spectrum became the primary focus of the final phase of the medicinal chemistry campaign. Herein is described the absorption, distribution, metabolism, and excretion (ADME) optimization effort that achieved this objective and culminated in the identification of **33**.

RESULTS AND DISCUSSION

During the earlier phases of the program, the PK properties of representative analogues from lead chemotypes with distinct

Table 2. Replicon and PK Assessments of Cap-Truncated Analogues 7-14[a]

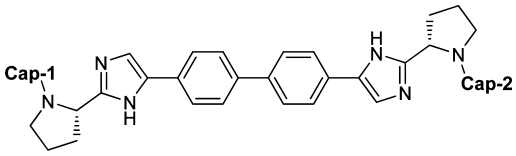

Compd	Cap-1	Cap-2	EC$_{50}$ (nM) GT-1a GT-1b	EC$_{50}$ (nM) BVDV	Solubility[b] (mg/mL)	PAMPA[b] (nm/s)	4 h PO Rat PK Screen[c] AUC (nM·h)	L-4 h (nM)	P-4 h (nM)
2[d]	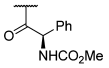	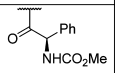	0.028 0.0067	1460	0.001	Null[e]	NC	ND	ND
7	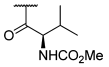	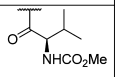	1240 1.22	3830	-	-	-	-	-
8[d]	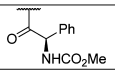	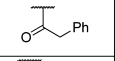	14.9 0.004	523	-	Null[e]	-	-	-
9	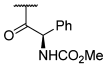	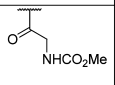	11.5 0.021	1370	0.005	164	NC	26.2	ND
10	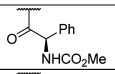	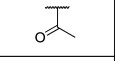	318 0.048	2530	0.006	500	-	-	-
11	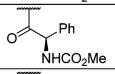	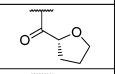	138 0.015	1710	0.008	464	809	2570	234
12	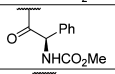	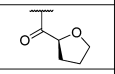	65.0 0.018	2250	0.007	480	127	802	27
13	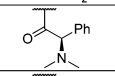	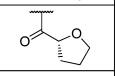	63.1 0.020	3420	>1.0	158	-	-	-
14	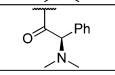	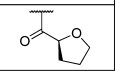	22.1 0.011	6500	0.49	200	62	563	27

[a]GT-1b CC$_{50}$ >10 μM for all except **9** (>8.1 μM). [b]Amorphous solubility and PAMPA values were determined at pH 6.5 and pH 7.4, respectively. [c]NC = not calculated; ND = not detected. [d]Reported previously in ref 6f. [e]Null = compound was not detected by UV plate reader in both the receiver and donor assay wells.

structural compositions were assessed; however, poor oral exposure was the most frequent observation. Early indications from in vitro studies including PAMPA permeability assays were that limited intestinal absorption, likely because of a combination of poor intrinsic permeability, poor pharmaceutical properties, and P-glycoprotein (P-gp) efflux, might be playing the dominant role in hampering systemic exposure. The aqueous solubility of carbamate **2** and amine **3**, when assessed using amorphous material, differed considerably, with marginal solubility (0.001 mg/mL) noted for **2** and excellent solubility (>0.61 mg/mL) for the more basic **3**. Thus, a decision was made to implement complementary structure−activity relationship (SAR) optimization strategies concurrently that involved examining both leads as part of a broader effort aimed at securing optimal exposure. The first approach focused primarily on improving the drug-like characteristics of the carbamate cap series, exemplified by **2**, by either increasing its solubility and/or reducing its molecular footprint, while the second dealt with improving the permeability properties of the amine cap series, exemplified by **3**, through modulation of electronic and steric parameters of the benzylic substituent (Figure 1).

As part of the initial SAR exploration, one of the phenyl groups of the biaryl core of **2** was replaced with six-membered heterocyclic analogues (Table 1). While the introduction of polarity to the central scaffold region of **2**, as in **4**−**6**, caused variable levels of loss in inhibitory potency toward both GT-1a (27- to 111-fold) and GT-1b (3- to 5-fold) replicons, there was an incremental gain in amorphous solubility when assessed in buffer at pH 6.5. In addition, measurable PAMPA values were observed, indicative of some level of intrinsic permeability. However, in rat PK assessments—either a 4 h screen or a 24 h study—**4** and **5** did not exhibit measurable systemic exposure after oral dosing, whereas **6** showed minimal plasma exposure (PO-AUC = 21 nM·h; F = 0.5%) but was not detected in either the liver or plasma at 24 h.[7]

It was reasoned that some degree of molecular weight reduction of the leads would be necessary to improve their exposure properties. With this in mind, an SAR optimization campaign was embarked upon to further delineate the balance that may exist between oral exposure and potency (Table 2). Replacing both of the phenylglycine caps of **2** with the unnatural enantiomer of valine, which retained the (*R*)-stereoconfiguration at the α-carbon, resulted in more than 40000-fold loss in GT-1a inhibitory activity (compare **7** and **2**). A lower but still significant loss in GT-1a inhibitory potency (410- to 11400-fold) was also observed when one of the caps of **2** was truncated, as in **8**−**10**. It is noteworthy that partial truncation had minimal impact on GT-1b antiviral potency, with EC$_{50}$ values ≤48 pM maintained by these analogues. Although compound **9** exhibited moderate PAMPA permeability and some gain in amorphous solubility, it had no meaningful exposure following oral dosing to rats. It soon

Table 3. Replicon and PK Assessment of Basic Cap Analogues 15−22

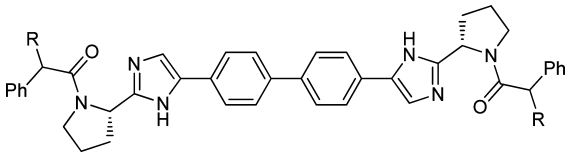

Compd	R/R[a]	EC_{50} (nM)		CC_{50} GT-1b (nM)	Solubility[b] (mg/mL)	PAMPA[b] (nm/s)	4 h PO Rat PK screen[c,d]		
		GT-1a GT-1b	BVDV				AUC (nM·h)	L-4 h (nM)	P-4 h (nM)
3[e]	NMe$_2$	0.037 0.042	2350	5860	>0.61	7	NC	ND	ND
15	NMeEt	0.029 0.017	1300	1840	>1.0	106	6	1976	2
16	NEt$_2$	0.043 0.016	1320	1850	>0.1	255	13	1089	6
17	N	0.060 0.046	448	954	>0.69	36	5	80	0.7
18	N	0.038 0.013	1200	2360	0.070	251	47	1205	13
19	N O	6.05 0.024	5880	>10^4	0.021	349	54	239	11
20	N F	2.61 0.020	8820	>10^4	0.042	Null[f]	-	-	-
21	N F	>1000 8.27	1340	>10^4	0.027	Null[f]	-	-	-
22	NEt$_2$ N	0.048 0.012	1370	2290	0.66	337	-	-	-

[a]Compound **20** and **21** are symmetrical diastereomers but with unknown stereochemistry at their benzylic center [i.e., either (*R*/*R*) or (*S*/*S*)], whereas the remaining compounds have (*R*/*R*)-stereoconfiguration. Compound **22** is a mixed-cap analogue. [b]Amorphous solubility and PAMPA values were determined at pH 6.5 and pH 7.4, respectively. [c]NC = not calculated; ND = not detected with the exception that one plasma sample obtained for **3** at 0.17 h indicated 20 nM concentration. [d]Estimated clearance (mL/min·kg) from 4 h IV rat PK screen (2 mg/kg dose; $n = 2$): **3** (17), **15** (88), **16** (4), **18** (58). [e]Reported previously in ref 6f. [f]Null = compound was not detected by UV plate reader in both the receiver and donor assay wells.

became apparent from structure−activity studies that maintaining a phenylglycine cap at one end of the molecule and varying the alternate cap region afforded mixed-cap analogues exhibiting GT-1a EC_{50} values near 100 nM but with notable improvements in PAMPA permeability compared to the progenitor **2**. Assessment of one such analogue, **11**, in a rat PK screen indicated a marked gain in exposure for the molecule (Table 2). Interestingly, compound **12**, a diastereomer of **11** with similar PAMPA permeability value, displayed a lower exposure in the rat. Compound **11** was advanced into additional rat, dog, and mouse PK studies in order to gather information on the cross-species exposure properties of the chemotype, and data is summarized in Table 4. In a 24 h rat PK study, **11** exhibited low clearance, a small volume of distribution, and a half-life of 6.9 h after IV dosing. After oral dosing, **11** exhibited low bioavailability (6.8%), a favorable liver/plasma ratio (26), and liver exposure at 24 h (116 nM) that is below its GT-1a EC_{50} (138 nM). In light of the compound's low IV clearance, its low bioavailability is believed to reflect incomplete absorption, attributed to P-gp efflux, a contention supported by results from in vitro Caco-2 bidirectional studies (**11**: A−B, <15 nm/s; B−A, 105 nm/s). Compound **11** showed higher oral bioavailability in the mouse (17%) and dog (45%) when compared to rat (6.8%). Although a follow-up study to probe into the reasons behind the noted differences in oral bioavailability was not conducted, it is noteworthy that there was evidence for enterohepatic recirculation in the mouse and dog, which may have favorably impacted the oral bioavailability in these species.

Compounds **13** and **14**, the dimethyl amine cap analogues of **11** and **12**, respectively, were prepared and profiled in standard in vitro and rat PK studies to gather comparative data on the two cap families in order to help chart a path forward. These compounds exhibited improved solubility, similar inhibitory activity in the GT-1a replicon, but lower PAMPA permeability, when compared with their carbamate counterparts **11** and **12**, respectively. In light of the multispecies PK data obtained for **11**, the amine cap analogue **13** was advanced directly to 24 h rat, dog, and mouse PK studies to establish a comparative benchmark for the two versions of the phenylglycinamide cap class. Compound **13** exhibited higher clearance and volume of distribution in all three species and a longer half-life in rat and mouse when compared to the carbamate counterpart **11**. After oral dosing to rats, **13** was not detected in the plasma or liver at 24 h; however, there was measurable systemic exposure in both the mouse and dog after PO dosing, although the absolute levels were lower than that of **11**. Enterohepatic recirculation was evident for **13** across species in both dosing arms, with

Table 4. PK Assessment of 11, 13, and 18 in Rats, Dogs, and/or Mouse[a,b]

		IV (24 h)			PO (24 h)			
compd	animal	CL (mL/min·kg)	Vd (L/kg)	$t_{1/2}$ (h)	AUC (nM·h)	L-24 h (nM)	P-24 h (nM)	% *F*
11	rat	4.4	0.3	6.9	1830	116	4.5	6.8%
	dog	22	7.5	>10	1520		6.0	45%
	mouse	5.3	1.9	2.9	15100	253	59	17%
13	rat	57	60	14	NC	ND	ND	
	dog	102	82	NC[c]	436		30	60%
	mouse	18	14	7.8	1422	539	25	6.0%
18	rat	63	20	7.7	NC	ND[d]	ND	
	dog	28	10	>12	272		8.3	14%

[a]Respective IV/PO dosing levels: rat (2/5 mg/kg), dog (1/3 mg/kg), mouse (5/20 mg/kg). Number of animals per dosing group: rat (n = 3), dog (n = 2), mouse (n = 9; composite design). Vehicle: PEG-400 for mouse-IV/PO, rat-IV/PO, and dog-PO; PEG-400/water (9:1) for dog-IV. [b]NC = not calculated; ND = not detected. [c]$t_{1/2}$ could not be calculated because of a rise in plasma level through 24 h. [d]Only 1 of 3 rats had a detectable level (318 nM).

rising plasma levels through 24 h in some cases, which introduced some variability to the data and complicated its interpretation. Interestingly, in comparing the rat PO exposure of **11** to **14**, there was no correlation between exposure and the stereoconfiguration of the tetrahydrofuran moiety, because for the carbamate cap pair **11** and **12**, the (*R*)-isomer exhibited the better exposure, whereas for the amine cap pair **13** and **14**, it was the (*S*)-isomer that showed higher exposure. Finally, as part of the effort to profile lead molecules of interest for off-target liabilities, **11** and **13** were assessed in a panel of biochemical screens conducted at a concentration of 10 μM by MDS Pharma and were found to inhibit the binding of a radioligand to the Na^+ channel site-2 by 82 and 102%, respectively. In a follow-up study conducted in-house, whole-cell patch-clamp analysis revealed that **11** and **13** inhibited Na^+ channel conductance by 14 and 53%, respectively, at a concentration of 10 μM in protein-free buffer at pH 7.4.

In a concurrent effort, a complementary SAR survey was conducted around the second lead, amine **3**, in order to determine the feasibility of improving its PK properties through modification of the steric and electronic properties of the benzylic amine substituent (Table 3). Consistent with SAR findings disclosed previously for the cap region when examined in the context of an anilide chemotype, there was broad tolerance to steric bulk around the benzylic site and that attenuation of the basicity of the amine group had a detrimental impact on GT-1a inhibitory potency (Table 3).[6e] For example, in modifying the dimethylamine moiety of **3** to a piperidine, as in **18**, the GT-1a and GT-1b inhibitory activities remained essentially unchanged, varying by <4-fold, whereas less basic analogues, morpholine **19** and fluoro-pyrrolidine **20**, exhibited a 44- to 101-fold diminished GT-1a antiviral activity when compared to pyrrolidine **17**. Following oral administration to rats monitored for 4 h, compounds **15**−**19** demonstrated low plasma exposure, with AUC values ranging from 5 to 54 nM·h, although the liver concentrations at 4 h surpassed 1.0 μM for three of the five (**15**, **16**, and **18**) analogues. Interestingly, although pyrrolidine **17** exhibited the lowest PAMPA permeability value and the poorest oral exposure among the derivatives of **3** advanced to rat PK studies, the reason why this molecule behaves significantly different from its close homologues **15**, **16**, and **18** is not readily apparent. A subset of the analogues were also assessed in an IV rat PK screen and the estimated clearance ranged from 4 mL/min·kg for **16** to 88 mL/min·kg for **15**.

For **15**, **16**, and **18**, the observed 4 h PO-liver exposure would provide more than a 25000-fold multiple over their GT-1a replicon EC_{50} values, which was much higher than that of compound **11**, 19-fold at 4 h. While the high exposure multiple achieved after oral dosing by the potent amine cap analogues in the targeted tissue was encouraging, their plasma 4 h AUC was >10-fold lower when compared with that of **11**. To gain additional insight into the PK properties of this series, **18** was advanced into more detailed 24 h rat and dog PK studies (Table 4). Compound **18** exhibited high clearance, a high volume of distribution, and a prolonged half-life in rats following IV dosing. After oral dosing, the compound was barely detectable in the plasma through 24 h, and only 1 of 3 rats exhibited liver exposure (318 nM) at 24 h. In dog PK studies, **18** showed moderate to high clearance, a high volume of distribution, a long half-life after IV dosing, and an oral bioavailability of 14%. As was the case for mixed-cap analogues **11** and **13** discussed earlier, the homodimeric analogue **18** exhibited better exposure in dogs than rats. It appears that oral exposure in rats for **18** was subject to considerable variability, a concern from developability perspective, but the likely cause for this observation was not investigated.

Compound **18** was characterized further in a select panel of in vitro assays designed to gather additional information about the potential off-target liabilities of analogues containing basic phenylglycine caps. In whole-cell patch-clamp assays, performed at a concentration of 10 μM, **18** inhibited Na^+, hERG, and Ca^{2+} channels by 94, 82, and 69%, respectively. While no glutathione (GSH) conjugate was detected following incubation of **18** with GSH-supplemented human and rat liver microsomes, a cyanide adduct was detected when KCN was used in place of GSH, an indication for the formation of a reactive metabolite. It is noteworthy that the mixed-cap analogue **22** exhibited cyanide addition only to the piperidine cap portion when subjected to a similar bioactivation study, an indication that related basic cap analogues may have differentiated liabilities.

There were a number of important findings from the in vitro and PK studies discussed above that proved instrumental in formulating an end-game strategy in search of a candidate exhibiting optimal virology, ADME, and safety properties. First, it was demonstrated that reduction of the overall molecular size of leads **2** and **3**, as in **11**, **12**, and **14**, significantly enhanced oral exposure. Moreover, both carbamate **12** and amine **14** exhibited exposure in a rat PK screen following oral solution dosing that were within 2-fold of each other, although the

Table 5. Replicon and PK Assessment of Non-Basic Cap-Truncated Analogues 23−31[a]

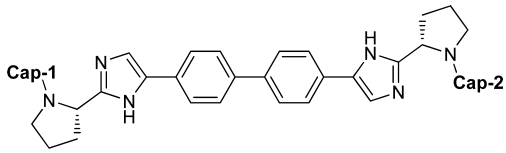

Compd	Cap-1	Cap-2	EC$_{50}$ (nM)		Solubility[b] (mg/mL)	PAMPA[b] (nm/s)	4 h PO Rat PK screen[c]		
			GT-1a GT-1b	BVDV			AUC (nM·h)	L-4 h (nM)	P-4 h (nM)
9	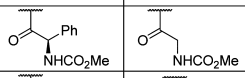		11.5 0.021	1370	0.005	164	NC	26.2	ND
23	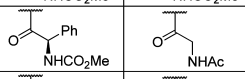		77.8 0.158	2040	0.014	12	-	-	-
24	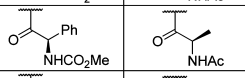		32.8 0.20	3320	-	28	-	-	-
25	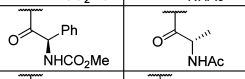		39.6 0.075	4190	0.028	100	-	-	-
26	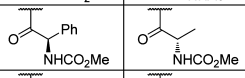		0.112 0.013	2160	0.008	363	-	-	-
27	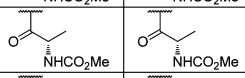		0.282 0.090	>10^4	0.060	207	281	134	57
28	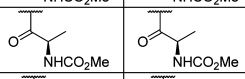		709 1.16	3580	0.036	47	-	-	-
29	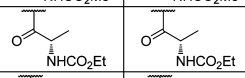		>123 4.35	>10^4	0.023	451	-	-	-
30	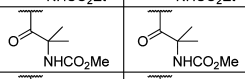		>123 191	6360	-	26	-	-	-
31	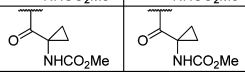		>123 3.91	>10^4	0.14	2	-	-	-

[a]GT-1b CC$_{50}$ >10 μM for all except **9** (>8.1 μM). [b]Amorphous solubility and PAMPA values were determined at pH 6.5 and pH 7.4, respectively. [c]NC = not calculated; ND = not detected.

potential advantage that the relatively more soluble **14** may have under nonsolution dosing by, for example, minimizing the likelihood of dissolution-rate limited absorption, was not investigated. In the case of the homodimeric amine cap series, although the liver exposure was favorably impacted by increases in lipophilicity, plasma exposure was low and variable. Second, a limited correlation was established between PAMPA permeability and oral exposure in rat PK screen for the chemotype. In addition, it was observed that rat was a more stringent PK model to guide the SAR evolution because the compounds that were advanced into dog and/or mouse PK studies hitherto (i.e., **11**, **13**, and **18**) demonstrated relatively enhanced oral bioavailabilities in those species. Finally, preliminary in vitro safety assessments revealed that analogues containing amine-based caps may possess increased liability for ion channel inhibition. Taken together, the carbamate series emerged as the more attractive class for additional optimization where a combination of PAMPA and rat PK screening were deemed sufficient to gauge progress toward compounds with targeted exposure. The key outstanding issue that needed to be addressed at this juncture was how to regain the significant (>4900-fold) GT-1a inhibitory potency that was lost in pursuit of improved PK properties in analogues such as **11**.

The next phase of the SAR exploration focused around carbamate **9** and the small set of related analogues **23**−**25** that were prepared as part of the initial cap truncation exercise (Table 5). While acetamides **23**−**25** had similar inhibitory potency toward GT-1a or GT-1b replicon, the introduction of a methyl group with the (*S*)-stereoconfiguration appeared to have impacted the PAMPA permeability favorably (compare **23** and **25**). Because carbamate **9** was among the most potent GT-1a inhibitors, EC$_{50}$ of 12 nM, within the cap-truncated analogues examined hitherto, its (*S*)-alanine variant was prepared in anticipation of enhanced PAMPA permeability. While changing the glycine cap of **9** to the (*S*)-alanine cap of **26** had the expected favorable impact on PAMPA permeability, this modification was also associated with a 100-fold enhancement of potency toward the GT-1a replicon, unanticipated based on the SAR that had been developed to date. Because it had been demonstrated previously that the GT-1a antiviral potency of mixed-cap analogues resided between that of the respective homodimeric cap analogues, the gain in the GT-1a inhibitory potency with **26** strongly suggested that the corresponding (*S*)-alanine cap homodimer would be very potent toward a GT-1a replicon, which indeed was the case (**27**: GT-1a EC$_{50}$ = 0.282 nM).[6f] Notably, and in line with the activity of *bis*-(*R*)-valine cap analogue **7** discussed earlier, the *bis*-(*R*)-alanine cap analogue **28** was >2000-fold weaker than its diastereomer **27** toward the GT-1a replicon. This result brought into clear focus a difference in stereochemical requirements at the α-carbon between the phenylglycine and the alkylglycine cap derivatives. Moreover, this finding demonstrated that the initial assumption made in retaining the (*R*)-stereoconfiguration during the cap truncation exercise

Table 6. Replicon and PK Assessment of Advanced Analogues 32−41[a]

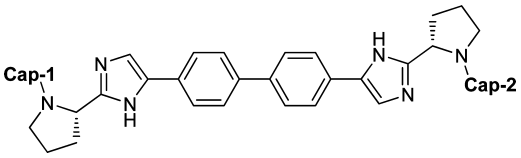

Compd	Cap-1	Cap-2	EC_{50} (nM) GT-1a GT-1b	EC_{50} (nM) BVDV	Solubility[b] (mg/mL)	PAMPA[b] (nm/s)	4 h PO Rat PK screen AUC (nM·h)	4 h PO Rat PK screen L-4 h (nM)	4 h PO Rat PK screen P-4 h (nM)
32			0.139 0.0113	>10^4	0.036	384	-	-	-
33[c]			0.050 0.009	9000	0.014	496	2181	2239	661
34			0.126 0.053	>10^4	0.063	275	472	453	121
35			0.145 0.026	>10^4	0.016	500	-	-	-
36			43.5 0.019	6130	-	-	-	-	-
37			>123 0.34	>10^4	-	-	-	-	-
38			762 2.0	3770	-	-	-	-	-
39			0.0364 0.0119	5610	>0.13	253	49	1826	30
40			0.0238 0.0058	7680	>1.0	363	NA[d]	471	NA[d]
41			0.0244 0.0059	4680	0.37	706	34	1233	13

[a]GT-1b CC_{50} >10 μM for all. [b]Amorphous solubility and PAMPA values were determined at pH 6.5 and pH 7.4, respectively. [c]Virology data reported previously in ref 2. [d]NA = not available. In 24 h rat PK study (IV/PO: 2/5 mg/kg; n = 3) **40** showed an oral bioavailability of 4.3%. Following oral dosing, it had a plasma AUC of 106 nM·h and a 24 h liver level of 132 nM, whereas it was not detected in the plasma at 24 h.

while going from *bis*-(*R*)-phenylglycine analogue **2** to *bis*-(*R*)-valine analogue **7**, although reasonable based on extant SAR, was incorrect.[8]

Securing subnanomolar GT-1a inhibitory potency in the alkylglycine cap series through stereochemical inversion was a critical milestone for the program because it allowed a reduction in the molecular size of the cap moiety and in the aromatic composition of the chemotype, translating into improved aqueous solubility and rat oral exposure (compare **27** vs **2**).[9] The follow-up effort focused on this new cap series in order to further enhance its exposure properties. Whereas the modifications illustrated in analogues **29**−**31** were detrimental to both GT-1a and GT-1b antiviral activity, incorporation of other aliphatic moieties at the α-carbon favorably impacted potency and/or PK, with compound **33** exhibiting the best combination of replicon potency and oral exposure in the rat PK screen among related analogues prepared in this final iteration of SAR study (Tables 5 and 6). Removal of the H-bond-donating capability of the carbamate moiety of **33**, as in **36**, caused a significant reduction in GT-1a inhibitory potency while having minimal impact on the antiviral effect in a GT-1b replicon. In addition, replacing the carbamate moiety of **33** with an acetamide, as in **37**, which retains H-bonding capability, was also detrimental to antiviral activity. Despite the apparent similarity in the carbamate pharmacophoric elements of the potent (*S*)-alkyl- and (*R*)-phenyl-glycine cap classes, their stereochemical disparity suggests that the respective carbamate moieties may engage the NS5A proteins in subtly different fashions.

In a parallel effort directed toward identifying alternate, structurally differentiated candidates with enhanced pharmaceutical properties, a select group of (*S*)-alkylglycine cap derivatives was hybridized with (*R*)-*N*,*N*-diethylphenylglycine to afford the mixed-cap analogues **39**−**41** (Table 6). This basic glycinamide cap was chosen over alternate variants (i.e., caps of **15** and **18**) because it demonstrated improved properties in earlier studies, including a lower estimated clearance in the rat IV PK screen and a decreased liability for bioactivation in an in vitro assay (see Table 3 and earlier discussions). Though the replicon potencies of **39**−**41** were comparable to that of homodimer **16**, the improvement in oral plasma exposure with **39** and **41** in a 4 h rat PK screen was more limited than was the case for **33**. Nevertheless, based on the preliminary virology profile and rat PK screen assessment results, **39** was selected for additional characterization along with *bis*-(*S*)-valine cap analogue **33**.

Compounds **33** and **39** exhibited potent inhibitory activities toward a broad panel of HCV genotypes, although **39** was more potent than **33** toward GT-2a and GT-3a strains (Table 7).[2,10] Compound **39** inhibited Na^+ and hERG channels in patch-clamp assays to a greater extent than **33**. In rat, dog, and cynomolgus monkey PK studies, **33** demonstrated higher oral

Table 7. Replicon and off-Target Liability Assessment of 33 and 39[a]

compd		33[b]	39
EC_{50} (nM)	GT-2a JFH-1	0.071	0.020
	GT-2a J6	7.5	0.99
	GT-3a	0.146	0.008
	GT-3a YH	364	59
	GT-3a YH*	1451	
	GT-4a	0.012	0.014
	GT-5a	0.033	0.021
	GT-6	0.054	
% inhibition of Na^+ channel at 10 μM		51%	62%
hERG IC_{50} (μM)		29.2	9.1

[a]Except for GT-2a JFH-1, all are hybrid replicons in either GT-2a JFH-1 or GT-1b Con1 backbone: GT-2a J6 (JFH-1); GT-3a or GT-3a YH (Con1); GT-3a YH* (JFH-1); GT-4a (Con1); GT-5a (JFH-1); GT-6a (JFH-1). [b]A subset of the replicon data of **33** has been reported previously in refs 2 and 10.

bioavailabilities, F = 38−108%, compared to **39**, F = 3.6−66%, and enhanced oral plasma exposure (Table 8). In order to further differentiate the two compounds, they were examined in a 4 day mouse toxicology study where male and female animals were administered doses of 15, 50, and 100 mg/kg orally on a QD regimen. Both compounds were well-tolerated, and there were no significant exposure differences between the genders. However, the 0−24 h plasma AUC and liver and heart exposures of **39**, sampled at 8 and 24 h, approximately doubled between day 1 and day 4 at each dose level while remaining unchanged, or slightly decreasing, for **33**. Based on these findings, **33** was deemed the preferred compound, and it was advanced through additional ADME characterization studies and an extensive array of standard in vitro and in vivo off-target liability assessments, including extended multispecies toxicology. The results of these studies supported its advancement into clinical trials.[11]

Table 8. Multispecies Oral 24 h PK Assessment of 33 and 39[a]

compd	animals	dose level (mg/kg)	AUC (μM·h)	P-24h (nM)	L-24h (nM)	% F
33	rat	5.0	4.8	18	103[b]	50%
	dog	2.3	11	26		108%
	monkey	2.8	1.93	6.5		38%
39	rat	5.0	0.165	ND[c]	178	3.6%
	dog	3.5	1.2	9.0		66%
	monkey	3.0	0.497	4.2		20.9%

[a]Number of animals: rat (3), dog (2), monkey (3). See the Experimental Section for details on vehicles. [b]L-24 h data is an average of 2 values since **33** was not detected in the liver of 1 of 3 rats. [c]ND = not detected.

Compound **33** was safe and well-tolerated when dosed as a solution at 1 to 200 mg to healthy volunteers in a placebo-controlled, double-blind phase I clinical study.[2] Plasma exposure above the protein-binding adjusted GT-1a EC_{90} of 0.38 nM was observed at all doses through 24 h. In single-ascending dose studies conducted in HCV-infected subjects, doses of 1, 10 and 100 mg of **33** were associated with a mean 1.8, 3.2, and 3.3 $\log_{10}$ reduction in viral RNA, respectively, measured 24 h post administration. The viral decline was more pronounced in two GT-1b-infected subjects that received the 100 mg dose, and, most notably, one of these subjects attained a viral titer below 25 IU/mL, the lower limit of quantification for the study. This rate and extent of decline of plasma HCV RNA following a single oral administration of a small molecule was unprecedented in the field of HCV therapeutics and provided clinical proof-of-concept for the efficacy of HCV NS5A replication complex inhibitors. In a 14 day multiple-ascending dose study, though a mean maximum decline in viral titer of 2.8 to 4.1 $\log_{10}$ was observed in subjects receiving doses of 1 to 100 mg QD or 30 mg BID of **33**, viral breakthrough occurred during treatment, indicating that the compound has a low genetic barrier to resistance.[12] The amino acid changes associated with the resistance correlated with those observed in the in vitro replicon assay. In this study, the antiviral response was relatively more pronounced in GT-1b- than GT-1a-infected subjects, where 4 of 7 GT-1b-infected subjects compared to none of the 17 GT-1a-infected subjects attained viral titers below 25 IU/mL at day 14.

Compound **33** is currently in phase II and III clinical trials in combination with other DAA agents targeting the orthogonal mechanism(s) and/or pegylated-interferon-α/ribavirin regimens.[13,14] A noteworthy finding from these studies is the demonstration that 24 weeks of therapy with a combination of **33** (60 mg QD) and the NS3/4A inhibitor asunaprevir (600 mg BID) was associated with a sustained viral response 24 weeks after cessation of therapy (SVR_{24}) of 36%, providing the first demonstration that HCV infection can be cured by a drug regimen that is free of pegylated-interferon-α and ribavirin.[13a] A dual DAA combination therapy involving **33** and asunaprevir for the treatment of GT-1b interferon-ineligible/-intolerant subjects or those that are nonresponders to interferon/ribavirin therapy has completed phase III studies. A request to market **33** and asunaprevir was filed with the Japanese regulatory agency in October 2013. In addition, a triple DAA combination of **33**, asunaprevir, and the NS5B polymerase inhibitor BMS-791325 is currently undergoing phase II evaluation for the treatment of HCV GT-1a/1b-infected subjects, with encouraging preliminary results.[15] In addition to the evolving clinical impact that **33** has been demonstrating in the HCV field, it has also served as a tool compound in a number of mode-of-action studies directed at deciphering the NS5A protein's various functions, an effort that has also shed some light on likely reasons behind the high inhibitory potency associated with the NS5A-targeting class of compounds.[16]

■ CHEMISTRY

Final compounds were readily prepared according to the synthetic routes highlighted in Schemes 1−3.[17] In the case of aza-core analogues **4**−**6**, key synthetic fragments **48a**, **48c**, and **52b** were initially assembled as illustrated in Scheme 1. Bromination of ketone **42**, followed by alkylation with Boc-L-proline and cyclization of the resultant ketoester **44** provided bromopyridine **48a**.[18] Regioselective lithiation of dibromopyridine **45a** followed by condensation with a Weinreb reagent furnished carbamate **46a**, which was elaborated to **48b** via the intermediacy of ketoamide **47**.[19] Bromoketone **50**, prepared from **45b** through a combination of a Stille coupling and in situ bromination, was elaborated to chloropyrimidine **52a** via ketoester **51**. Whereas **48a** was coupled with boronate **53** under standard Suzuki-Miyaura condition to provide **54a**, applying a similar condition to **48b** or **52a** was not successful (Scheme 2). However, protection of their imidazole moiety with SEM ether, as in **48c** and **52b**, facilitated the Suzuki-

Scheme 1. Preparation of Intermediates 48a, 48c, and 52b[a]

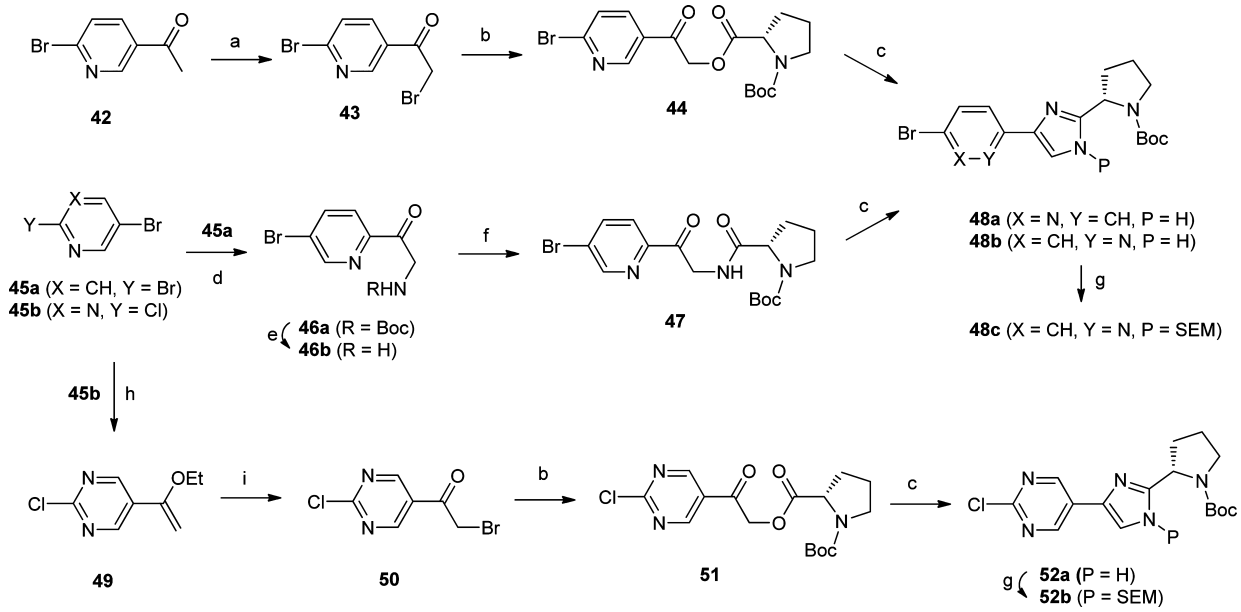

[a]Reagents and conditions: (a) Br_2, HBr, CH_2Cl_2; (b) *N*-Boc-L-proline, Et_3N, CH_3CN; (c) NH_4OAc, xylenes, 140 °C; (d) *n*-BuLi, *t*-butyl 2-(methoxy(methyl)amino)-2-oxoethylcarbamate; −78 °C to −15 °C; (e) 48% HBr, dioxane; (f) *N*-Boc-L-proline, HATU, DIEA, DMF; (g) NaH, SEM-Cl, DMF; (h) tributyl(1-ethoxyvinyl)tin, $PdCl_2(Ph_3P)_2$, DMF, 100 °C; (i) NBS, H_2O/THF, 0 °C.

Scheme 2. Preparation of Aza-Core Analogues 4−6[a]

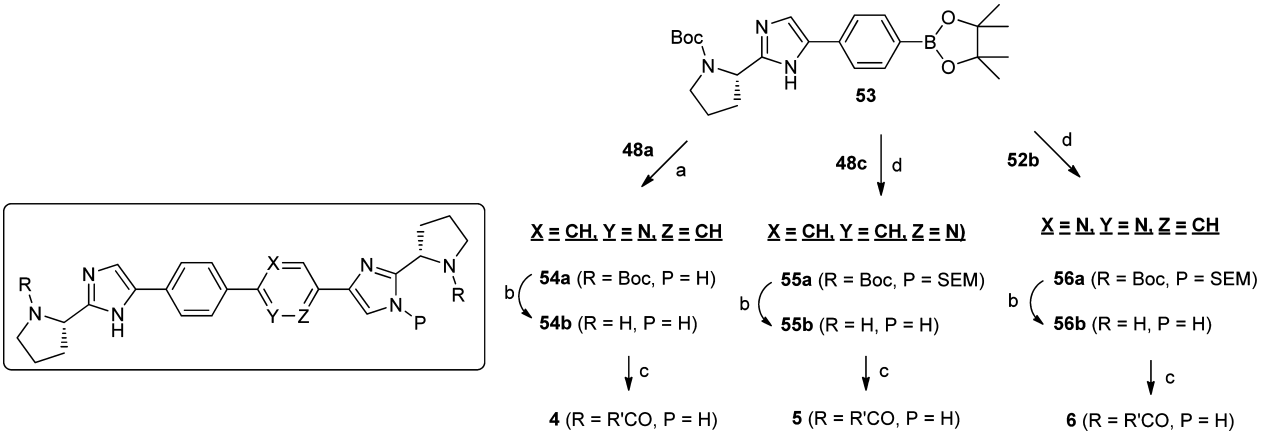

[a]Reagents and conditions: (a) $Pd(Ph_3P)_4$, $NaHCO_3$, DME/H_2O, 90 °C; (b) 25% TFA/CH_2Cl_2; (c) (2*R*)-2-[(methoxycarbonyl)amino]-2-phenylacetic acid, HATU, DIEA, DMF; (d) $Pd(Ph_3P)_4$, $NaHCO_3$, DME/H_2O, 80 °C.

Miyaura coupling. It is noteworthy that the regiochemistry of the SEM ethers was not determined. Acid-catalyzed deprotection of intermediates **54a**, **55a**, and **56a**, followed by coupling of the resultant pyrrolidines with (2*R*)-2-[(methoxycarbonyl)amino]-2-phenylacetic acid under standard HATU/DIEA condition provided final products **4**−**6** (Scheme 2). Homodimeric and mixed-cap analogues of the *bis*-phenylimidazole template were prepared from **57a** and **57b**, respectively, according to general routes described previously (see Scheme 3).[2,6f] The majority of the cap moieties used for the final step were prepared readily from commercially available precursors through adaptation of literature protocols.[17] For a subset of the cases, such as compounds **11**−**14**, the cap precursors were obtained from vendors.

CONCLUSION

In summary, distinct strategies were implemented toward enhancing the oral exposure of two lead series of the *bis*-phenylimidazole class of HCV NS5A replication complex inhibitor, represented by the carbamate cap analogue **2** and the amine cap analogue **3**. Although the application of different approaches favorably impacted the oral exposure properties of both series to varying degrees, the more promising PK findings resulted from a cap-truncation exercise that was performed in the context of **2**. The mixed-cap analogue **11** emerged from this approach as a molecule with improved PK, but the structural modification unfortunately resulted in >4900-fold loss in GT-1a inhibitory potency. It was the combination of PAMPA permeability and 4 h rat PK screen studies that guided additional SAR exploration toward achieving balanced virology and oral exposure properties. An unexpected finding with

Scheme 3. Preparation of Homodimeric and Mixed-Cap Analogues[a]

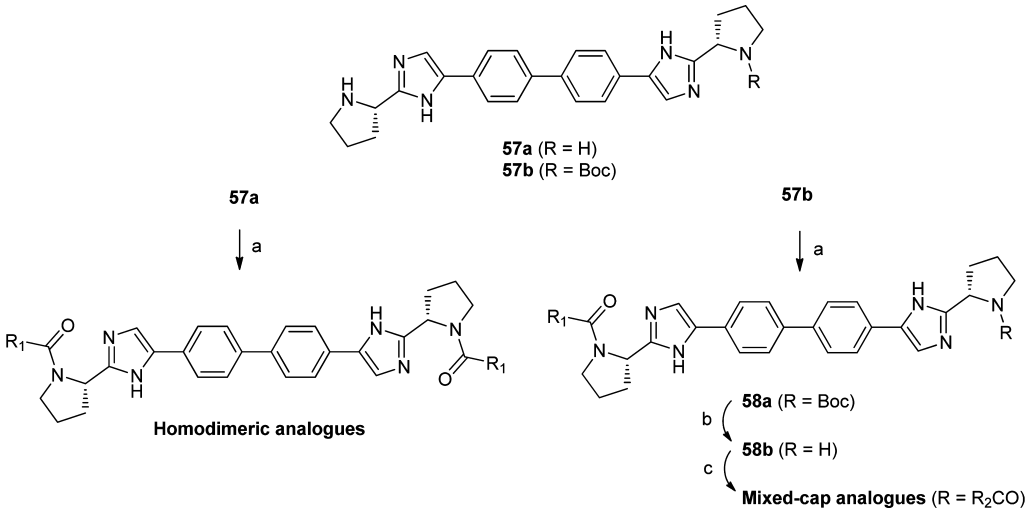

[a]Reagents and conditions: (a) R_1CO_2H, HATU, DIEA, DMF; (b) 25% TFA/CH_2Cl_2 or 4 N HCl/dioxane; (c) R_2CO_2H, HATU, DIEA, DMF.

Table 9. LC/MS Conditions for the Characterization of Final Products

method	columns	gradient and run time	flow rate (mL/min)	solvent A	solvent B
1	1	10−100% B; 70 min	0.35	A1	B1
2	2	10−100% B; 70 min	0.4	A2	B2
3	1	10−100% B; 70 min	0.3	A1	B2
4	3	10−50% B; 40 min	0.3	A2	B2
		50−100% B; 40−70 min			
5	4	10−100% B; 70 min	0.4	A1	B2
6	5	10−50% B; 25 min	0.5	A1	B2
		50−100% B; 25−32 min			
7	6	0−100% B; 3 min	4	A3	B3
8	7	0−100% B; 3 min	4	A3	B3
9	7	0−100% B; 2 min	4	A3	B3
10	8	0−100% B; 2 min	4	A4	B4
11	9	0−100% B; 4 min	0.8	A3	B3
12	10	0−100% B; 4 min	0.8	A3	B3
13	6	0−100% B; 4 min	4	A3	B3

Columns: column 1: Waters Atlantis C18 (2.1 × 150 mm, 3.5 μm); column 2: Agilent Zorbax Extend C18 (2.0 × 150 mm, 5 μm); column 3: Agilent Zorbax Extend C18 (2.1 × 150 mm, 3.5 μm); column 4: Waters Sunfire C18 (2.1 × 150 mm, 3.5 μm); column 5: Acquity UPLC BEH C18 (2.1 × 100 mm, 1.7 μm); column 6: Phenomenex-Luna C18 (4.6 × 50 mm, S10); column 7: Phenomenex Luna C18 (3.0 × 50 mm, S10); column 8: Primesphere C18-HC (4.6 × 30 mm); column 9: Phenomenex-Luna C18 (2.0 × 50 mm, 3 μm); column 10: Xbridge Phenyl (2.1 × 50 mm, 2.5 μm). Solvent A: solvent A1 = 25 mM NH_4OAc in water at pH = 5; solvent A2 = 30 mM NH_4HCO_3 in water at pH = 10; solvent A3 = 0.1% TFA in 10% MeOH/90% H_2O; solvent A4 = 5 mM NH_4OAc in 10% CH_3CN/90% H_2O. Solvent B: solvent B1 = 25 mM NH_4OAc in 85% CH_3CN/15% H_2O; solvent B2 = CH_3CN; solvent B3 = 0.1% TFA in 90% MeOH/10% H_2O; solvent B4 = 5 mM NH_4OAc in 90% CH_3CN/10% H_2O.

respect to the stereochemical requirement of the two carbamate cap series was uncovered that provided the opportunity to replace the arylglycine cap of **2** with an alkylglycine analog, enabling the identification of **33**. Notable direct-acting antiviral therapies in clinical development nearing fruition contain NS5A replication complex inhibitors.[20]

■ EXPERIMENTAL SECTION[21]

Reactions were conducted, purified, and analyzed according to methods widely practiced in the field, while taking necessary precautions in the exclusion of moisture and/or oxygen where appropriate. Final compounds were tested as either TFA salts or free base. Although, where relevant, the exact TFA content was not determined, its mole equivalent was assumed to be equal to the number of basic moieties residing in the molecule for purposes of yield and EC_{50} calculations. LC/MS analyses were performed on a Shimadzu LC instrument coupled to a Waters Micromass ZQ instrument or Waters 2795 HPLC with Micromass ZQ MS (electrospray probe) and Waters 996 PDA detection. All tested compounds exhibited >95% purity under the LC conditions provided in Table 9. HRMS analyses were conducted on a Thermo Scientific Finnegan MAT900 or Fourier Transform Orbitrap spectrometers, calibrated daily. NMR spectra were recorded on a Bruker Ultrashield 400 MHz spectrometer or on a Bruker Advance-III 500 MHz spectrometer, each equipped with a 5 mm TXI cryoprobe. Residual protio-solvent was used as internal standard for chemical shift assignments. Coupling constants are provided in Hz, with the following spectral pattern designations: s, singlet; d, doublet; t, triplet; q, quartet; quint, quintet; dd, doublet of doublets; dt, doublet of triplets; m, multiplet; br, broad; app, apparent. ^{1}H NMR analyses of most intermediates and final

products in DMSO-d_6 at ambient temperature indicated the presence of rotamers and/or tautomers and that the chemical shift provided is for the dominant rotamer(s) and/or tautomer(s).

Abbreviations used in the experimental descriptions: DIEA, *N*,*N*-diisopropylethylamine; EtOAc, ethyl acetate; HATU, 1-[bis(dimethylamino)methylene]-1*H*-1,2,3-triazolo[4,5-b]-pyridinium 3-oxid hexafluorophosphate; MeOH, methanol; satd. aq, saturated aqueous; RT, room temperature.

Methyl *N*-[(1*R*)-2-[(2*S*)-2-{5-[6-(4-{2-[(2*S*)-1-[(2*R*)-2-[(methoxycarbonyl)amino]-2-phenylacetyl]pyrrolidin-2-yl]-1*H*-imidazol-5-yl}phenyl)pyridin-3-yl]-1*H*-imidazol-2-yl}pyrrolidin-1-yl]-2-oxo-1-phenylethyl]carbamate (4). A solution of Br_2 (7.63 g, 47.74 mmol) in CH_2Cl_2 (10 mL) was added dropwise over 5 min to an ice water cooled solution of 1-(6-bromopyridine-3-yl)ethanone (9.496 g, 47.47 mmol) and 48% HBr (0.4 mL) in CH_2Cl_2 (105 mL). The cooling bath was removed 40 min later, and stirring was continued at ambient temperature for 66 h. The cake of solid that formed was filtered, washed with CH_2Cl_2, and dried in vacuo to afford impure bromide **43** as an off-white solid (15.94 g), which was carried forward directly.

Boc-L-proline (9.70 g, 45.06 mmol) was added in one batch to a heterogeneous mixture of crude **43** (15.4 g) and CH_3CN (150 mL), followed immediately by Et_3N (13.0 mL, 93.2 mmol), which was added dropwise over 6 min. The reaction mixture was stirred for 50 min, the volatile component was removed in vacuo, and the residue was partitioned between CH_2Cl_2 and H_2O. The CH_2Cl_2 layer was dried ($MgSO_4$), filtered, and concentrated in vacuo, and the residue was purified by flash chromatography (silica gel; sample was loaded with eluting solvent; 25% EtOAc/hexanes) to afford ketoester **44** as a highly viscous yellow oil (11.44 g, 61%). ^{1}H NMR (400 MHz, DMSO-d_6): δ 8.95 (m, 1H), 8.25−8.21 (m, 1H), 7.88 (d, J = 8.3, 1H), 5.65−5.46 (m, 2H), 4.36−4.31 (m, 1H), 3.41−3.29 (m, 2H), 2.36−2.22 (m, 1H), 2.14−2.07 (m, 1H), 1.93−1.83 (m, 2H), 1.4/1.36 (2 s, 9H). LC/MS (ESI) m/z: $[M + Na]^+$ calcd for $C_{17}H_{21}NaBrN_2O_5$, 435.1; found, 435.2. HRMS (ESI) m/z: $[M + H]^+$ calcd for $C_{17}H_{22}BrN_2O_5$, 413.0712; found, 413.0717.

A mixture of **44** (1.32 g, 3.19 mmol) and NH_4OAc (2.729 g, 35.4 mmol) in xylenes (18 mL) was heated in a microwave at 140 °C for 90 min. The volatile component was removed in vacuo, and the residue was partitioned between CH_2Cl_2 and H_2O, where enough satd. aq $NaHCO_3$ solution was added to neutralize the aqueous medium. The aqueous phase was extracted with CH_2Cl_2, and the combined organic phase was dried ($MgSO_4$), filtered, and concentrated in vacuo. The residue was purified by flash chromatography (silica gel; 50% EtOAc/hexanes) to afford imidazole **48a** as an off-white foam (1.025 g, 82%). ^{1}H NMR (400 MHz, DMSO-d_6): δ 12.33/12.09/12.02 (series of br s, 1H), 8.74 (d, J = 2.3 Hz, 0.93H), 8.70 (app br s, 0.07H), 8.03/7.98 (dd for the first peak, J = 8.3, 2.6 Hz, 1H), 7.69/7.67 (2 overlapping app br s, 1H), 7.58/7.43 (d for the first peak, J = 8.3 Hz, 1H), 4.80 (m, 1H), 3.53 (m, 1H), 3.36 (m, 1H), 2.33−2.11 (m, 1H), 2.04−1.79 (m, 3H), 1.39/1.15 (2 br s, 3.9H+5.1H). LC/MS (ESI) m/z: $[M + H]^+$calcd for $C_{17}H_{22}BrN_4O_2$, 393.1; found, 393.2. HRMS (ESI) m/z: $[M + H]^+$ calcd for $C_{17}H_{22}BrN_4O_2$, 393.0926; found, 393.0909.

$Pd(Ph_3P)_4$ (115 mg, 0.100 mmol) was added to a mixture of **48a** (992 mg, 2.52 mmol), **53** (see ref 2 for preparation; 1.207 g, 2.747 mmol), $NaHCO_3$ (698.8 mg, 8.318 mmol) in 1,2-dimethoxyethane (18 mL) and H_2O (4 mL). The reaction mixture was flushed with N_2, heated at 90 °C for 37 h using an oil bath, and allowed to cool to RT. The suspension that formed was filtered and washed with H_2O followed by 1,2-dimethoxyethane, and dried in vacuo. A silica gel mesh was prepared from the crude solid and submitted to flash chromatography (silica gel, EtOAc) to afford **54a** as a white solid, which yellowed slightly upon standing at RT (1.124 g, ∼68%). ^{1}H NMR indicated that the sample contained residual MeOH in a product/MeOH mole ratio of 1.3. LC/MS (ESI) m/z: $[M + H]^+$ calcd for $C_{35}H_{44}N_7O_4$, 626.4; found, 626.6. HRMS (ESI) m/z: $[M + H]^+$ calcd for $C_{35}H_{44}N_7O_4$, 626.3455; found, 626.3479.

Carbamate **54a** (217 mg) was treated with 25% TFA/CH_2Cl_2 (3.6 mL) and stirred at RT for 6 h. The volatile component was removed in vacuo, and the resultant material was free-based by MCX column (MeOH wash; 2.0 M NH_3/MeOH elution) to afford **54b** as a dull, yellow foam that solidified gradually after it was allowed to stand with no processing (150.5 mg; mass is above theoretical yield). ^{1}H NMR (400 MHz, DMSO-d_6): δ 11.89 (br s, 2H), 9.01 (d, J = 1.8 Hz, 1H), 8.13 (dd, J = 8.3, 2.2 Hz, 1H), 8.07 (d, J = 8.6 Hz, 2H), 7.92 (d, J = 8.3 Hz, 1H), 7.83 (d, J = 8.5 Hz, 2H), 7.61 (br s, 1H), 7.50 (br s, 1H), 4.18 (m, 2H), 3.00−2.93 (m, 2H), 2.90−2.82 (m, 2H), 2.11−2.02 (m, 2H), 1.94−1.85 (m, 2H), 1.83−1.67 (m, 4H). Note: the exchangeable pyrrolidine hydrogens were not observed. LC/MS (ESI) m/z: $[M + H]^+$ calcd for $C_{25}H_{28}N_7$: 426.2; found, 426.4. HRMS (ESI) m/z: $[M + H]^+$ calcd for $C_{25}H_{28}N_7$, 426.2406; found, 426.2425.

To a mixture of **54b** (23.2 mg, ∼0.0512 mmol), (2*R*)-2-[(methoxycarbonyl)amino]-2-phenylacetic acid (24.4 mg, 0.117 mmol), DIEA (40 μL, 0.229 mmol) in DMF (1.5 mL) was added HATU (41.9 mg, 0.110 mmol). The mixture was stirred at RT for 1 h and directly submitted to a reverse-phase preparative HPLC purification (MeOH/H_2O/TFA) to afford the TFA salt of **4** as an off-white foam (43.4 mg, 74%). ^{1}H NMR (400 MHz, DMSO-d_6): δ 14.33 (br s, ∼1H), 9.15−8.95 (series of m, 1H), 8.57−8.51 (m, 0.15H), 8.40−8.04 (m, 5.6H), 8.04−7.92 (m, 1.55H), 7.92−7.76 (m, 0.72H), 7.76−7.66 (m, 1.66H), 7.46−7.25 (m, 9.01H), 7.25−7.10 (m, 0.16H), 7.10−6.94 (m, 1.15H), 5.76−5.63 (2 m, 0.15H), 5.57−5.37 (2 m, 1.97H), 5.26−5.13 (m, 1.88H), 3.99−3.88/3.88−3.74 (2 m, 2H), 3.74−3.66/3.23−3.09 (2 m, 2H), 3.55/3.53 (2 s, 6H), 2.34−2.17 (m, 1.75H), 2.14−1.97 (m, 3.85H), 1.97−1.75 (m, 2.4H). LC (method 1): t_R = 31.3 min. LC/MS (ESI) m/z: $[M + H]^+$ calcd for $C_{45}H_{46}N_9O_6$, 808.4; found, 808.5. HRMS (ESI) m/z: $[M + H]^+$ calcd for $C_{45}H_{46}N_9O_6$, 808.3571; found, 808.3576.

Methyl *N*-[(1*R*)-2-[(2*S*)-2-{5-[5-(4-{2-[(2*S*)-1-[(2*R*)-2-[(methoxycarbonyl)amino]-2-phenylacetyl]pyrrolidin-2-yl]-1*H*-imidazol-5-yl}phenyl)pyridin-2-yl]-1*H*-imidazol-2-yl}pyrrolidin-1-yl]-2-oxo-1-phenylethyl]carbamate (5). *n*-BuLi (12.0 mL of 2.5 M in hexanes, 30 mmol) was added dropwise over 15 min to a cooled (−78 °C) semisolution of 2,5-dibromopyridine (**45a**) (6.040 g, 25.5 mmol) in toluene (300 mL), and the reaction mixture was stirred for 2.5 h. *t*-Butyl 2-(methoxy(methyl)amino)-2-oxoethylcarbamate (2.809 g, 12.87 mmol) was added in batches over 7 min, and the mixture was stirred for 1.5 h at −78 °C. The cooling bath was replaced with a −60 °C bath, which was allowed to warm up to −15 °C over 2.5 h. The reaction mixture was quenched with satd. aq NH_4Cl solution (20 mL) and allowed to thaw to ambient temperature. The organic layer was separated and

concentrated in vacuo. The crude product was purified by flash chromatography (silica gel, 15% EtOAc/hexanes) to afford a reddish-brown semisolid, which was washed with hexanes to remove some colored residue. Pyridine **46a** was isolated as an ash-colored solid (842 mg, 21%). ^{1}H NMR (400 MHz, DMSO-d_6): δ 8.89 (d, J = 2.3 Hz, 1H), 8.30 (dd, J = 8.4, 2.4 Hz, 1H), 7.90 (d, J = 8.3 Hz, 1H), 7.03(br t, J = 5.7 Hz, 0.88H), 6.63 (app br s, 0.12H), 4.55 (d, J = 5.8 Hz, 2H), 1.40/1.28 (2 app s, 7.83H/1.17H). LC/MS (ESI) m/z: [M + Na]$^+$ calcd for $C_{12}H_{15}BrNaN_2O_3$, 337.0; found, 337.1.

HBr (48%, 1.0 mL) was added dropwise to a solution of **46a** (840 mg, 2.66 mmol) in dioxane (5.0 mL) over 3 min, and the reaction mixture was stirred at RT for 17.5 h. The precipitate was filtered, washed with dioxane, and dried in vacuo to afford the HBr salt of **46b** as an off-white solid (672.4 mg; the precise mole equivalent of HBr was not determined). ^{1}H NMR (400 MHz, DMSO-d_6): δ 8.95 (d, J = 2.3 Hz, 1 H), 8.37 (dd, J = 8.4, 2.3 Hz, 1H), 8.20 (br s, 3H), 8.00 (d, J = 8.3 Hz, 1H), 4.61 (s, 2H). LC/MS (ESI) m/z: [M + H]$^+$ calcd for $C_7H_8BrN_2O$, 215.0; found, 215.0.

DIEA (2.3 mL, 13.2 mmol) was added dropwise over 15 min to a heterogeneous mixture of **46b** (1.365g), (S)-Boc-proline (0.957 g, 4.44 mmol) and HATU (1.70 g, 4.47 mmol) in DMF (13.5 mL), and the mixture was stirred at RT for 1 h. The volatile component was removed in vacuo, and the residue was partitioned between EtOAc (40 mL) and an aqueous medium (20 mL H_2O + 1 mL satd. aq $NaHCO_3$). The aqueous layer was washed with EtOAc (20 mL), and the combined organic phase was dried ($MgSO_4$), filtered, and concentrated in vacuo. The residue was purified by flash chromatography (silica gel; 40−50% EtOAc/hexanes) to afford **47** as a light-yellow foam (1.465g). ^{1}H NMR (400 MHz, DMSO-d_6): δ 8.90 (d, J = 2.3 Hz, 1H), 8.30 (dd, J = 8.5, 2.4 Hz, 1H), 8.21−8.07 (m, 1H), 7.90 (d, J = 8.3 Hz, 1H), 4.80−4.69 (m, 1H), 4.64 (dd, J = 19.1, 5.5 Hz, 1H), 4.24−4.10 (m, 1H), 3.43−3.33 (m, 1H), 3.33−3.26 (m, 1H), 2.20−2.01 (m, 1H), 1.95−1.70 (m, 3H), 1.40/1.35 (2 app s, 9H). LC/MS (ESI) m/z: [M + Na]$^+$ calcd for $C_{17}H_{22}BrN_3NaO_4$, 434.1; found, 434.0.

A mixture of **47** (782.2 mg, 1.897 mmol) and NH_4OAc (800.0 mg, 10.4 mmol) in xylenes (10 mL) was heated in a microwave (140 °C) for 90 min. The volatile component was removed in vacuo, and the residue was carefully partitioned between CH_2Cl_2 and H_2O, where enough satd. aq $NaHCO_3$ was added to neutralize it. The aqueous phase was extracted with CH_2Cl_2 (2×), and the combined organic phase was dried ($MgSO_4$), filtered, and concentrated in vacuo. The crude material was purified by flash chromatography (silica gel; 50% CH_2Cl_2/EtOAc) to afford **48b** as an off-white solid (552.8 mg, 74%). ^{1}H NMR (400 MHz, DMSO-d_6): δ 12.49/12.39/12.15/12.06 (series of br s, 1H), 8.62 (app br s, 0.2H), 8.56 (d, J = 2.0 Hz, 0.8H), 8.02 (br d, J = 8.5 Hz, 0.2H), 7.97 (br d, J = 7.8 Hz, 0.8H), 7.77 (d, J = 8.6 Hz, 0.8H), 7.72 (d, J = 8.6 Hz, 0.2H), 7.61−7.49 (m, 1H), 4.93−4.72 (m, 1H), 3.53 (m, 1H), 3.41−3.32 (m, 1H), 2.33−1.77 (m, 4H), 1.39 (app s, 3.7H), 1.14/1.12 (2 overlapped app s, 5.3H). LC/MS (ESI) m/z: [M + Na]$^+$ calcd for $C_{17}H_{21}BrN_4NaO_2$, 415.1; found, 415.1.

NaH (60% dispersion in mineral oil; 11.6 mg, 0.29 mmol) was added in one portion to a heterogeneous mixture of **48b** (80 mg, 0.20 mmol) and DMF (1.5 mL), and stirred at RT for 30 min. SEM-Cl (40 μL, 0.23 mmol) was added dropwise over 2 min to the reaction mixture, and stirring was continued for 14 h. The volatile component was removed in vacuo and the residue was partitioned between H_2O and CH_2Cl_2. The aqueous layer was extracted with CH_2Cl_2, and the combined organic phase was dried ($MgSO_4$), filtered, and concentrated in vacuo. The crude material was purified by flash chromatography (silica gel; 20% EtOAc/hexanes) to afford **48c** as a colorless viscous oil (87.5 mg, 84%). The exact regiochemistry of **48c** was not determined, as it was deemed inconsequential for the current purpose. ^{1}H NMR (400 MHz, $CDCl_3$): δ 8.53 (d, J = 2.2 Hz, 1H), 7.91−7.82 (m, 1H), 7.82−7.72 (m, 1H), 7.52 (s, 1H), 5.87 (m, 0.46H), 5.41 (m, 0.54H), 5.16 (d, J = 10.8 Hz, 1H), 5.03−4.85 (m, 1H), 3.76−3.42 (series of m, 4H), 2.54−1.84 (series of m, 4H), 1.38/1.19 (2 br s, 4.3H/4.7H), 0.97−0.81 (m, 2H), −0.03 (s, 9H). LC/MS (ESI) m/z: [M + H]$^+$ calcd for $C_{23}H_{36}BrN_4O_3Si$, 523.2; found, 523.2.

$Pd(Ph_3P)_4$ (24.4 mg, 0.021 mmol) was added to a mixture of **48c** (280 mg, 0.535 mmol), **53** (see ref 2 for preparation; 241.5 mg, 0.55 mmol) and $NaHCO_3$ (148.6 mg, 1.769 mmol) in 1,2-dimethoxyethane (4.8 mL) and H_2O (1.6 mL). The reaction mixture was flushed with N_2, heated with an oil bath at 80 °C for ∼24 h, and then the volatile component was removed in vacuo. The residue was partitioned between CH_2Cl_2 and H_2O, and the organic phase was dried ($MgSO_4$), filtered, and concentrated in vacuo. The crude material was purified by flash chromatography (silica gel; 75−100% EtOAc/hexanes) followed by a reverse-phase preparative HPLC (H_2O/MeOH/TFA). The HPLC elute was neutralized with 2 M NH_3/MeOH and evaporated in vacuo, and the residue was partitioned between H_2O and CH_2Cl_2. The organic layer was dried ($MgSO_4$), filtered, and concentrated in vacuo to afford **55a** as a white foam (162 mg, 40%). LC/MS (ESI) m/z: [M + H]$^+$ calcd for $C_{41}H_{58}N_7O_5Si$, 756.4; found, 756.6.

Carbamate **55a** (208 mg, 0.275 mmol) was treated with 25% TFA/CH_2Cl_2 (4.0 mL), and the mixture was stirred at RT for 10 h. The volatile component was removed in vacuo, and the residue was first free-based by MCX (MeOH wash; 2.0 M NH_3/MeOH elution) and then purified by a reverse-phase preparative HPLC (H_2O/MeOH/TFA), and the resultant material was free-based again (MCX) to afford **55b** as a film of oil (53.7 mg, 46%). ^{1}H NMR (400 MHz, DMSO-d_6): δ 11.86 (app br s, ∼2H), 8.83 (d, J = 2.1 Hz, 1H), 8.07 (dd, J = 8.3, 2.3 Hz, 1H), 7.87 (d, J = 8.5 Hz, 1H), 7.84 (d, J = 8.3 Hz, 2H), 7.71 (d, J = 8.3 Hz, 2H), 7.55 (s, 1H), 7.50 (br s, 1H), 4.20−4.15 (m, 2H), 3.00−2.94 (m, 2H), 2.89−2.83 (m, 2H), 2.11−2.02 (m, 2H), 1.95−1.86 (m, 2H), 1.83−1.67 (m, 4H). Note: the exchangeable pyrrolidine hydrogens were not observed. LC/MS (ESI) m/z: [M + H]$^+$ calcd for $C_{25}H_{28}N_7$, 426.2; found, 426.3.

Title compound **5** (TFA salt, off-white foam) was prepared from **55b** and (2R)-2-[(methoxycarbonyl)amino]-2-phenylacetic acid according to the procedure described for **4**. ^{1}H NMR (400 MHz, DMSO-d_6): δ 14.32 (br s, ∼1H), 9.14−9.00 (m, 1H), 8.45−8.34 (m, 1.82H), 8.30−8.23 (m, 0.15H), 8.23−8.13 (app s, 1.04H), 8.13−7.93 (series of m, 4.81H), 7.93−7.76 (m, 0.72H), 7.76−7.60 (m, 1.5H), 7.44−7.27 (m, 9.08H), 7.07−6.98 (m, 0.88H), 5.75−5.68 (m, 0.12H), 5.57−5.45 (m, 1.6H), 5.45−5.35 (m, 0.34H), 5.26−5.12 (m, 1.94H), 3.99−3.87/3.87−3.77 (2 m, 2H), 3.77−3.66/3.23−3.06 (2 m, 2H), 3.55/3.53 (2 s, 6H), 2.32−2.16 (m, 1.8H), 2.16−1.96 (m, 4H), 1.96−1.75 (m, 2.2H). LC (method 2): t_R = 24.0 min. LC/MS (ESI) m/z: [M + H]$^+$ calcd for $C_{45}H_{46}N_9O_6$, 808.36; found, 808.51.

Methyl *N*-[(1*R*)-2-[(2*S*)-2-{5-[4-(5-{2-[(2*S*)-1-[(2*R*)-2-[(methoxycarbonyl)amino]-2-phenylacetyl]pyrrolidin-2-yl]-1*H*-imidazol-5-yl}pyrimidin-2-yl)phenyl]-1*H*-imida-

zol-2-yl}pyrrolidin-1-yl]-2-oxo-1-phenylethyl] carbamate (6). Tributyl(1-ethoxyvinyl)tin (10.0 mL, 29.6 mmol) and $PdCl_2(Ph_3P)_2$ (1.04 g, 1.48 mmol) were added to a mixture of **45b** (5.72 g, 29.6 mmol) in DMF (80 mL) maintained under an atmosphere of N_2. The mixture was heated at 100 °C for 3 h before being allowed to stir at RT for 16 h. The reaction mixture was diluted with Et_2O (200 mL) and treated with aqueous KF solution (25 g of KF in 150 mL of water). The two-phase mixture was stirred vigorously for 1 h at RT and filtered through Celite. The organic phase of the filtrate was separated, washed with saturated $NaHCO_3$ solution, brine and dried (Na_2SO_4). The original aqueous phase was extracted twice with Et_2O, and the combined organic extract was treated as above. The crude product was preabsorbed onto silica gel and purified by flash chromatography (silica gel, 3−50% EtOAc/hexanes) to afford **49** (6.1 g) as a white solid which was slightly impure but was used as is. ^{1}H NMR (500 MHz, DMSO-d_6): δ 8.97 (s, 2H), 5.08 (d, J = 3.7 Hz, 1H), 4.56 (d, J = 3.4 Hz, 1H), 3.94 (q, J = 7.0 Hz, 2H), 1.35 (t, J = 7.0 Hz, 3H). LC/MS (ESI) m/z: $[M + H]^+$ calcd for $C_8H_{10}ClN_2O$, 185.1; found, 185.0. HRMS (ESI) m/z: $[M + H]^+$ calcd for $C_8H_{10}ClN_2O$, 185.0482; found, 185.0490.

NBS (3.37 g, 19.0 mmol) was added in one portion to a stirred solution of **49** (3.5 g, ∼19.0 mmol) in THF (53 mL) and H_2O (17.5 mL) at 0 °C under N_2. The mixture was stirred for 1 h at 0 °C before it was diluted with H_2O and extracted with EtOAc (2×). The combined extract was washed with satd. aq $NaHCO_3$, brine and dried (Na_2SO_4) to afford **50** (4.69 g) as a pale yellow solid, which was advanced to the next step without purification. LC/MS (ESI) m/z: $[M + H]^+$ calcd for $C_6H_5BrClN_2O$, 236.93; found, 236.78.

Crude **50** (4.69 g) was dissolved in anhydrous CH_3CN (150 mL) and treated directly with *N*-Boc-L-proline (4.08 g, 19.0 mmol) and DIEA (3.30 mL, 19.0 mmol). After being stirred for 3 h, the solvent was removed in vacuo, and the residue was partitioned between EtOAc and H_2O. The organic phase was washed with 0.1 N HCl, satd. aq $NaHCO_3$, brine and dried (Na_2SO_4) to afford crude **51**, which was advanced to the next step without purification.

Crude **51** was taken up in xylenes (60 mL) and treated with NH_4OAc (14.6 g, 190 mmol). The mixture was heated at 140 °C for 2 h in a pressure vessel before it was cooled to RT and suction-filtered. The filtrate was concentrated in vacuo, and the residue was partitioned between EtOAc and satd. aq $NaHCO_3$. The organic phase was separated, washed with brine, and dried over Na_2SO_4. Purification of the residue by flash chromatography (silica gel, 5−40% B/A, where A = CH_2Cl_2 and B = 25% MeOH/CH_2Cl_2) afforded **52a** as a pale, yellow foam (2.0 g, 30% yield for three steps). ^{1}H NMR (500 MHz, DMSO-d_6): δ 12.24−12.16 (m, 1H), 9.05 (s, 2H), 7.84−7.73 (m, 1H), 4.90−4.73 (m, 1H), 3.59−3.46 (m, 1H), 3.41−3.31 (m, 1H), 2.32−2.12 (m, 1H), 2.03−1.77 (m, 3H), 1.39/1.15 (2 s, 9H). LC/MS (ESI) m/z: $[M + H]^+$ calcd for $C_{16}H_{21}ClN_5O_2$, 350.1; found, 350.2. HRMS (ESI) m/z: $[M + H]^+$ calcd for $C_{16}H_{21}ClN_5O_2$, 350.1384; found, 350.1398.

NaH (60% dispersion in mineral oil; 0.23 g, 5.72 mmol) was added in one portion to a stirred solution of **52a** (2.00 g, 5.72 mmol) in dry DMF (45 mL) at RT under N_2. The mixture was stirred for 5 min, and SEM-chloride (1.00 mL, 5.65 mmol) was added gradually in 0.1 mL increments. The mixture was stirred for 3 h, quenched with satd. aq NH_4Cl, and diluted with EtOAc. The organic phase was separated, washed with satd. aq $NaHCO_3$, brine and dried (Na_2SO_4). The original aqueous phase was extracted with EtOAc (2×), and the combined extracts were washed with satd. aq $NaHCO_3$, brine and dried (Na_2SO_4). The residue was purified by flash chromatography (silica gel, 5−100% EtOAc/hexanes) to furnish **52b** as a pale yellow foam (2.35 g, 87%). Note that the exact regiochemistry of **52b** was not determined as it was deemed inconsequential for the current purpose. ^{1}H NMR (500 MHz, DMSO-d_6): δ 9.04 (s, 2H), 7.98−7.95 (m, 1H), 5.70−5.31 (3 m, 2H), 5.02−4.91 (m, 1H), 3.59−3.49 (m, 3H), 3.45−3.35 (m, 1H), 2.30−2.08 (m, 2H), 1.99−1.83 (m, 2H), 1.36/1.12 (2 s, 9H), 0.93−0.82 (m, 2H), −0.02 (s, 9H). LC/MS (ESI) m/z: $[M+H]^+$ calcd for $C_{22}H_{35}ClN_5O_3Si$, 480.2; found, 480.2. HRMS (ESI) m/z: $[M+H]^+$ calcd for $C_{22}H_{35}ClN_5O_3Si$, 480.2198; found, 480.2194.

$Pd(PPh_3)_4$ (0.12 g, 0.103 mmol) was added in one portion to a stirred suspension of **53** (see ref 2 for preparation; 1.00 g, 2.27 mmol), **52b** (0.99 g, 2.06 mmol), and $NaHCO_3$ (0.87 g, 10.3 mmol) in a solution of DME (20 mL) and H_2O (6 mL) at RT under N_2. The vessel was sealed and the mixture was heated at 80 °C with stirring for 16 h before additional $Pd(PPh_3)_4$ (0.12 g) was added. After being heated at 80 °C for an additional 12 h, the mixture was cooled to RT, diluted with EtOAc, washed with satd. aq $NaHCO_3$, brine and dried (Na_2SO_4). The volatile component was removed in vacuo. Purification of the residue by flash chromatography (silica gel, 40−100% EtOAc/hexanes) furnished **56a** as a yellow foam (1.53 g). A sample of the yellow foam was further purified for characterization purposes by reverse-phase preparative HPLC ($CH_3CN/H_2O/NH_4OAc$) to afford a pure sample as a white solid. ^{1}H NMR (500 MHz, DMSO-d_6): δ 12.30−11.88 (3 m, 1H), 9.17−9.16 (m, 2H), 8.43−8.31 (m, 2H), 7.99−7.35 (series of m, 4H), 5.72−5.30 (3 m, 2H), 5.03−4.76 (2 m, 2H), 3.64−3.50 (m, 4H), 3.48−3.31 (m, 2H), 2.36−2.07 (m, 2H), 2.05−1.80 (m, 4H), 1.46−1.08 (2 m, 18H), 0.95−0.84 (m, 2H), −0.01 (s, 9H). LC/MS (ESI) m/z: $[M + H]^+$ calcd for $C_{40}H_{57}N_8O_5Si$, 757.4; found, 757.4. HRMS (ESI) m/z: $[M + H]^+$ calcd for $C_{40}H_{57}N_8O_5Si$, 757.4221; found, 757.4191.

TFA (8.0 mL) was added in one portion to a stirred solution of **56a** (1.50 g, ∼1.98 mmol) in dry CH_2Cl_2 (30 mL) at RT. The flask was sealed, and the mixture was stirred for 16 h before the volatile component was removed in vacuo. The residue was dissolved in MeOH and purified by a reverse-phase preparative HPLC (MeOH/water/TFA). The desired fraction was concentrated, and the product was dissolved in MeOH and passed through a resin cartridge (UCT-CHQAX1 Quartnery amine hydroxide; MeOH elution) to afford the free-base form of **56b** as a pale, mustard yellow-colored solid (307 mg, 36%). ^{1}H NMR (500 MHz, DMSO-d_6): δ 12.50−11.80 (br m, 2H), 9.18 (s, 2H), 8.36 (d, J = 8.5 Hz, 2H), 7.89 (d, J = 8.2 Hz, 2H), 7.77 (s, 1H), 7.61 (s, 1H), 4.34−4.24 (m, 2H), 3.09−2.89 (m, 4H), 2.18−2.07 (m, 2H), 2.02−1.89 (m, 2H), 1.88−1.72 (m, 4H). Note: the exchangeable pyrrolidine hydrogens were not observed. LC/MS (ESI) m/z: $[M + H]^+$ calcd for $C_{24}H_{27}N_8$, 427.2; found, 427.0. HRMS (ESI) m/z: $[M + H]^+$ calcd for $C_{24}H_{27}N_8$, 427.2359; found, 427.2363.

To a solution of **56b** (60.0 mg, 0.14 mmol), (2*R*)-2-[(methoxycarbonyl)amino]-2-phenylacetic acid (64.8 mg, 0.31 mmol), and DIEA (0.20 mL, 1.1 mmol) in DMF (3.5 mL) was added HATU (123.0 mg, 0.32 mmol). The reaction mixture was stirred at RT for 2 h. It was then diluted with MeOH (2 mL), filtered through a Whatman 13 mm PVDF 45 μm syringe filter, and purified by reverse-phase preparative HPLC ($MeOH/H_2O/TFA$) to afford the TFA salt of **6** as a light

yellow solid (91.4 mg, 63% yield assuming bis-TFA salt). ^{1}H NMR (500 MHz, DMSO-d_6): δ 9.29/9.22/9.16 (3 s, 2H), 8.60−8.50 (m, 2H), 8.23 (app s, 0.77H), 8.16−8.08 (m, 0.87H), 8.01−7.65 (series of m, 4.27H), 7.44−7.27 (series of m, 8.8H), 7.05 (app s, 0.97H), 7.00−6.93 (m, 0.32H), 5.75−5.69 (m, 0.09H), 5.62−5.57 (m, 0.19H), 5.55−5.47 (m, 1.52H), 5.43−5.37 (m, 0.42H), 5.23−5.11 (m, 1.78H), 3.98−3.87 (m, 2H), 3.55/3.54/3.53 (3 s, 6H), 3.23−3.05 (m, 2H), 2.33−2.23 (m, 1H), 2.23−2.12 (m, 0.9H), 2.12−1.95 (m, 4H), 1.95−1.72 (m, 2.1H). LC (method 7): t_R = 1.99 min. LC/MS (ESI) m/z: [M + H]$^+$calcd for $C_{44}H_{45}N_{10}O_6$, 809.4; found, 809.2. HRMS (ESI) m/z: [M + H]$^+$ calcd for $C_{44}H_{45}N_{10}O_6$, 809.3524; found, 809.3505.

General Synthesis Description for Analogues of the Biphenyl Core Series. Homodimeric cap analogues were prepared from pyrrolidine **57a** and appropriate acid precursors according to the procedure described in the synthesis of **4**. The mixed-cap analogues were prepared from mono-Boc protected **57b** through a sequence involving coupling with the first cap, deprotecting the Boc moiety, and then installing the second cap, the details of which are provided in ref 6f. Depending on the HPLC eluting medium, final products were isolated as either TFA salt or free-base form.

Methyl *N*-[(2*R*)-1-[(2*S*)-2-{5-[4-(4-{2-[(2*S*)-1-[(2*R*)-2-[(methoxycarbonyl)amino]-3-methylbutanoyl]-pyrrolidin-2-yl]-1*H*-imidazol-5-yl}phenyl)phenyl]-1*H*-imidazol-2-yl}pyrrolidin-1-yl]-3-methyl-1-oxobutan-2-yl]carbamate (7). Title compound **7** (TFA salt, white solid). ^{1}H NMR (500 MHz, DMSO-d_6): δ 14.35 (br s, ∼3H), 8.14 (app br s, 1.83H), 8.02−7.93 (m, 3.77H), 7.93−7.85 (m, 4.59H), 7.60 (app br s, 0.18H), 7.25 (d, J = 8.2 Hz, 1.59H), 6.77 (app br s, 0.04H), 5.87 (app br s, 0.24H), 5.18 (dd, J = 8.1, 3.8 Hz, 1.76H), 4.19 (app t, J = 7.8 Hz, 1.71H), 3.96−3.84 (m, 1.77H), 3.77−3.64 (m, 2.2H), 3.57/3.57 (2 overlapping s, 6H), 3.53−3.47 (m, 0.32H), 2.47−2.28 (m, 2.2H), 2.22−1.87 (series of m, 7.58H), 1.86−1.66 (m, 0.22H), 0.91 (d, J = 7.0 Hz, 4.9H), 0.87 (d, J = 6.7 Hz, 5.4H), 0.73 (d, J = 6.7 Hz, 0.9H), 0.40 (app br s, 0.8H). LC (method 8): t_R = 2.0 min. LC/MS (ESI) m/z: [M + H]$^+$ calcd for $C_{40}H_{51}N_8O_6$, 739.4; found, 739.7. HRMS (ESI) m/z: [M + H]$^+$ calcd for $C_{40}H_{51}N_8O_6$, 739.3932; found, 739.3966.

Methyl *N*-[(1*R*)-2-[(2*S*)-2-{5-[4-(4-{2-[(2*S*)-1-{2-[(methoxycarbonyl)amino]acetyl}pyrrolidin-2-yl]-1*H*-imidazol-5-yl}phenyl)phenyl]-1*H*-imidazol-2-yl}-pyrrolidin-1-yl]-2-oxo-1-phenylethyl] carbamate (9). Title compound **9** (TFA salt, off-white foam). ^{1}H NMR (500 MHz, DMSO-d_6): δ 14.44 (br s, ∼3H), 8.13 (app br s, 1.76H), 8.00−7.87 (2 m, 7.7H), 7.87−7.67 (series of m, 1.51H), 7.44−7.21 (series of m, 5.45H), 7.05 (app s, 0.51H), 6.83 (app br s, 0.07H), 5.71 (app br s, 0.09H), 5.54−5.49 (m, 0.83H), 5.43−5.37 (m, 0.23H), 5.23−5.26 (m, 1.85H), 3.95−3.89 (m, 1.7H), 3.89−3.80 (m, 1.2H), 3.78−3.68 (m, 1.23H), 3.64−3.56 (m, 0.94H), 3.55/3.53/3.49 (3 s overlapped with m, 6.28H), 3.22−3.14 (m, 0.65H), 2.46−2.32 (m, 1.36H), 2.32−2.17 (m, 0.82H), 2.12−1.96 (m, 4.52H), 1.98−1.83 (m, 1.3H). LC (method 3): t_R = 24.5 min. LC/MS (ESI) m/z: [M + H]$^+$ calcd for $C_{40}H_{43}N_8O_6$, 731.4; found, 731.4. HRMS (ESI) m/z: [M + H]$^+$ calcd for $C_{40}H_{43}N_8O_6$, 731.3306; found, 731.3333.

Methyl *N*-[(1*R*)-2-[(2*S*)-2-{5-[4-(4-{2-[(2*S*)-1-acetylpyrrolidin-2-yl]-1*H*-imidazol-5-yl}phenyl)phenyl]-1*H*-imidazol-2-yl}pyrrolidin-1-yl]-2-oxo-1-phenylethyl]carbamate (10). Title compound **10** (TFA salt, off-white foam). ^{1}H NMR (400 MHz, DMSO-d_6): δ 14.48 (br s, ∼3H), 8.23−8.11 (m, 1.84H), 8.04−7.89 (m, 7.88H), 7.89−7.67 (m, 1.23H), 7.46−7.26 (m, 4.56H), 7.05 (s, 0.49H), 5.76 (m, 0.05H), 5.57−5.48 (m, 0.75H), 5.44−5.36 (m, 0.27H), 5.24−5.12 (m, 1.93H), 4.01−3.85 (m, 1H), 3.82−3.67 (m, 1H), 3.64−3.53 (m, 1.31H), 3.52 (s, 2.94H), 3.22−3.07 (m, 0.75H), 2.44−2.22 (2 m, 2.25H), 2.13−1.85 (series of m with s at 2.04, 8.75H). LC (method 9): t_R = 1.32 min. LC/MS (ESI) m/z: [M + H]$^+$ calcd for $C_{38}H_{40}N_7O_4$, 658.3; found, 658.4. HRMS (ESI) m/z: [M + H]$^+$ calcd for $C_{38}H_{40}N_7O_4$, 658.3142; found, 658.3135.

Methyl *N*-[(1*R*)-2-oxo-2-[(2*S*)-2-{5-[4-(4-{2-[(2*S*)-1-[(2*R*)-oxolane-2-carbonyl]pyrrolidin-2-yl]-1*H*-imidazol-5-yl}-phenyl)phenyl]-1*H*-imidazol-2-yl}pyrrolidin-1-yl]-1-phenylethyl]carbamate (11). Title compound **11** (TFA salt, off-white foam). ^{1}H NMR (500 MHz, DMSO-d_6): δ 14.46 (br s, ∼3H), 8.17/8.15 (2 overlapping app s, 1.63H), 8.11−8.01 (m, 0.34H), 8.01−7.94 (m, 3.57H), 7.94−7.88 (m, 3.94H), 7.88−7.65 (series of m, 1.51H), 7.44−7.27 (series of m, 4.54H), 7.05 (app s, 0.47H), 5.78−5.71 (m, 0.08H), 5.59−5.48 (m, 0.93H), 5.43−5.37 (m, 0.16H), 5.25−5.12 (m, 1.83H), 4.64 (dd, J = 7.9, 5.2 Hz, 0.89H), 4.29 (app t, J = 6.6 Hz, 0.11H), 3.98−3.90 (m, 0.81H), 3.90−3.62 (series of m, 3.25H), 3.62−3.44 (m, 1.17H), 3.54/3.53 (2 s overlapped with m of same region, 3H), 3.24−3.11 (m, 0.77H), 2.47−2.33 (m, 1.36H), 2.33−2.22 (m, 0.8H), 2.22−2.11 (m, 1.03H), 2.11−1.98 (m, 4.48H), 1.98−1.87 (m, 2.03H), 1.87−1.77 (m, 2H), 1.77−1.64 (m, 0.30H). LC (method 2): t_R = 22.5 min. LC/MS (ESI) m/z: [M + H]$^+$ calcd for $C_{41}H_{44}N_7O_5$, 714.3; found, 714.4. HRMS (ESI) m/z: [M + H]$^+$ calcd for $C_{41}H_{44}N_7O_5$, 714.3404; found, 714.3430.

Methyl *N*-[(1*R*)-2-oxo-2-[(2*S*)-2-{5-[4-(4-{2-[(2*S*)-1-[(2*S*)-oxolane-2-carbonyl]pyrrolidin-2-yl]-1*H*-imidazol-5-yl}-phenyl)phenyl]-1*H*-imidazol-2-yl}pyrrolidin-1-yl]-1-phenylethyl]carbamate (12). Title compound **12** (TFA salt, off-white foam). ^{1}H NMR (500 MHz, DMSO-d_6): δ 14.51 (br s, ∼3H), 8.16/8.12 (2 app br s, 2.04H), 8.01−7.93 (m, 3.89H), 7.93−7.87 (m, 3.74H), 7.87−7.65 (series of m, 1.36H), 7.45−7.25 (m, 4.52H), 7.05 (app s, 0.45H), 5.77−5.67 (m, 0.06H), 5.59−5.49 (m, 0.94H), 5.42−5.39 (m, 0.15H), 5.24−5.14 (m, 1.85H), 4.64 (app dd, J = 7.8, 5.3 Hz, 0.74H), 4.54−4.48 (m, 0.26H), 3.99−3.88 (m, 0.98H), 3.88−3.65 (m, 3.64H), 3.54/3.53 (2 overlapping s, 3H), 3.50−3.33 (m, 0.75H), 3.23−3.12 (m, 0.63H), 2.45−2.12 (m, 3.52H), 2.12−1.97 (m, 4.82H), 1.97−1.86 (m, 1.21H), 1.86−1.78 (m, 1.56H), 1.78−1.69 (m, 0.89H). LC (method 2): t_R = 22.2 min. LC/MS (ESI) m/z: [M + H]$^+$ calcd for $C_{41}H_{44}N_7O_5$, 714.34; found, 714.24.

(2*R*)-2-(Dimethylamino)-1-[(2*S*)-2-{5-[4-(4-{2-[(2*S*)-1-[(2*R*)-oxolane-2-carbonyl]pyrrolidin-2-yl]-1*H*-imidazol-5-yl}phenyl)phenyl]-1*H*-imidazol-2-yl}pyrrolidin-1-yl]-2-phenylethan-1-one (13). Title compound **13** (TFA salt, light yellow solid). ^{1}H NMR (500 MHz, DMSO-d_6): δ 14.55 (br s, ∼3H), 10.24 (br s, ∼1H), 8.14 (app s, 1H), 8.07 (app br s, 1H), 8.00−7.85 (m, 7.73H), 7.72 (app br s, 0.29H), 7.67−7.53 (m, 4.46H), 7.28−7.08 (m, 0.52H), 5.77 (app br d, J = 7.3 Hz, 0.10H), 5.57 (app br d, J = 9.2 Hz, 0.12H), 5.49 (app br s, 0.11H), 5.45 (app s, 0.89H), 5.26−5.14 (m, 1.78H), 4.63 (app dd, J = 7.9, 5.2 Hz, 0.89H), 4.28 (app t, J = 6.4 Hz, 0.11H), 4.06−3.97 (m, 0.86H), 3.90−3.74 (m, 2.80H), 3.74−3.62 (m, 0.29H), 3.62−3.53 (m, 0.92H), 3.53−3.40 (m, 0.13H), 3.12−3.00 (m, 1H), 3.00−2.68 (2 overlapping br s, 3H), 2.57−2.11 (m overlapping with DMSO signal, ∼3.7H), 2.30−2.11 (2 m, 2.1H), 2.11−1.98 (m, 4.6H), 1.981−1.67 (series of m, 4.6H). LC (method 2): t_R = 21.6 min. LC/MS (ESI) m/z: [M + H]$^+$

calcd for $C_{41}H_{46}N_7O_3$, 684.4; found, 684.8. HRMS (ESI) *m/z*: [M + H]$^+$ calcd for $C_{41}H_{46}N_7O_3$, 684.3662; found, 684.3671.

(2*R*)-2-(Dimethylamino)-1-[(2*S*)-2-{5-[4-(4-{2-[(2*S*)-1-[(2*S*)-oxolane-2-carbonyl]pyrrolidin-2-yl]-1*H*-imidazol-5-yl}phenyl)phenyl]-1*H*-imidazol-2-yl}pyrrolidin-1-yl]-2-phenylethan-1-one (14). Title compound **14** (TFA salt, off-white foam). ^{1}H NMR (400 MHz, DMSO-d_6): δ 14.51 (br s, ∼1H), 10.24 (br s, ∼1H), 8.11/8.09 (2 overlapping s, 1.10H), 8.03 (br s, 0.80H), 7.98−7.84 (m, 7.04H), 7.84−7.63 (m, 0.94H), 7.63−7.52 (m, 4.16H), 7.27−7.08 (m, 0.96H), 5.75 (m, 0.07H), 5.57 (m, 0.11H), 5.49−5.42 (m, 1H), 5.23−5.15 (m, 1.82H), 4.64 (app dd, *J* = 7.7, 5.4 Hz, 0.86H), 4.54−4.48 (m, 0.14H), 4.07−3.95 (m, 0.86H), 3.86−3.70 (overlapping m, 3.74H), 3.48−3.39 (m, 0.21H), 3.34−3.25 (m, 0.19H), 3.07−2.97 (m, 1H), 2.96−2.88 (app br s, 0.34H), 2.82−2.54 (app br s, 4.66H), 2.44−2.32 (m, 1.6H), 2.30−2.11 (m, 1.4H), 2.11−1.96 (m, 6.4H), 1.96−1.65 (series of m, 3.6H). LC (method 4): t_R = 25.7 min. LC/MS (ESI) *m/z*: [M + H]$^+$ calcd for $C_{41}H_{46}N_7O_3$, 684.4; found, 684.5. HRMS (ESI) *m/z*: [M + H]$^+$ calcd for $C_{41}H_{46}N_7O_3$, 684.3662; found, 684.3692.

(2*R*)-2-[Ethyl(methyl)amino]-1-[(2*S*)-2-{5-[4-(4-{2-[(2*S*)-1-[(2*R*)-2-[ethyl(methyl)amino]-2-phenylacetyl]-pyrrolidin-2-yl]-1*H*-imidazol-5-yl}phenyl)phenyl]-1*H*-imidazol-2-yl}pyrrolidin-1-yl]-2-phenylethan-1-one (15). Title compound **15** (TFA salt, yellow foam). ^{1}H NMR (400 MHz, DMSO-d_6): δ 10.13/9.85 (2 overlapping br s, ∼2H), 8.05 (app br s, 1.77H), 7.96−7.83 (m, 7.63H), 7.76−7.69 (m, 0.47H), 7.69−7.61 (m, 3.49H), 7.61−7.45 (m, 5.37H), 7.45−7.35 (m, 0.21H), 7.23−7.08 (m, 1.06H), 5.91 (app br s, 0.06H), 5.75 (m, 0.09H), 5.52/5.46 (2 overlapping app br s, 2H), 5.24−5.17 (m, 1.85H), 4.12−3.89 (m, 1.65H), 3.89−3.75 (m, 0.2H), 3.68−3.53 (m, 0.15H), 3.47−2.65 (series of overlapping br m, ∼7.5H), 2.55−2.15 (series of m partially overlapped with DMSO signal, ∼6.5H), 2.15−1.97 (m, 3.75H), 1.97−1.81 (m, 2H), 1.18−1.74 (m, 0.25H), 1.38−1.10 (m, 6H). LC (method 9): t_R = 1.10 min. LC/MS (ESI) *m/z*: [M + H]$^+$ calcd for $C_{48}H_{55}N_8O_2$, 775.4; found, 775.5. HRMS (ESI) *m/z*: [M + H]$^+$ calcd for $C_{48}H_{55}N_8O_2$, 775.4448; found, 775.4456.

(2*R*)-2-(Diethylamino)-1-[(2*S*)-2-{5-[4-(4-{2-[(2*S*)-1-[(2*R*)-2-(diethylamino)-2-phenylacetyl]pyrrolidin-2-yl]-1*H*-imidazol-5-yl}phenyl)phenyl]-1*H*-imidazol-2-yl}-pyrrolidin-1-yl]-2-phenylethan-1-one (16). Title compound **16** (TFA salt, yellow foam). ^{1}H NMR (400 MHz, DMSO-d_6): δ 9.81 (br s, ∼2H), 8.13−7.98 (m, 1.8H), 7.98−7.81 (m, 7.4H), 7.81−7.76 (m, 0.3H), 7.76−7.63 (m, 3.85H), 7.63−7.43 (m, 5.59H), 7.28−7.08 (m, 1.06H), 6.02−5.94 (m, 0.2H), 5.60−5.51 (m, 0.26H), 5.44 (s, 1.76H), 5.21−5.11 (m, 1.78H), 4.18−4.01 (m, 1.59H), 3.86−3.79 (m, 0.15H), 3.67−3.54 (m, 0.13H), 3.35−2.79 (series of overlapping br m, 7.13H), 2.69−2.56 (m, 1H), 2.56−2.40 (m overlapped with DMSO signal, ∼2H), 2.29−2.14 (m, 1.84H), 2.14−1.98 (m, 3.89H), 1.98−1.80 (m, 1.95H), 1.80−1.65 (m, 0.32H), 1.37−0.94 (overlapping br m, 12H). LC (method 9): t_R = 1.12 min. LC/MS (ESI) *m/z*: [M + H]$^+$ calcd for $C_{50}H_{59}N_8O_2$, 803.5; found, 803.6. HRMS (ESI) *m/z*: [M + H]$^+$ calcd for $C_{50}H_{59}N_8O_2$, 803.4761; found, 803.4728.

(2*R*)-2-Phenyl-1-[(2*S*)-2-{5-[4-(4-{2-[(2*S*)-1-[(2*R*)-2-phenyl-2-(pyrrolidin-1-yl)acetyl]pyrrolidin-2-yl]-1*H*-imidazol-5-yl}phenyl)phenyl]-1*H*-imidazol-2-yl}pyrrolidin-1-yl]-2-(pyrrolidin-1-yl)ethan-1-one (17). Title compound **17** (TFA salt, off-white solid). ^{1}H NMR (400 MHz, DMSO-d_6 with D_2O exchange) δ 8.06 (s, 1.77H), 7.97−7.82 (m, 7.47H), 7.71−7.50 (m, 9.35H), 7.50−7.35 (m, 0.37H), 7.24−7.09 (2 m, 1.04H), 5.79−5.73 (m, 0.2H), 5.50 (s, 0.25H), 5.44 (s, 1.75H), 5.24−5.17 (m, 1.8H), 4.04−3.95 (m, 1.77H), 3.88−3.79 (m, 0.23H), 3.75−2.6 (series of overlapping br m, ∼9H), 2.60−2.36 (m overlapped with DMSO signal, ∼1H), 2.30−2.13 (m, 2H), 2.13−1.60 (m, 14H). LC (method 4): t_R = 36.9 min. LC/MS (ESI) *m/z*: [M + H]$^+$ calcd for $C_{50}H_{55}N_8O_2$, 799.44; found, 799.67.

(2*R*)-2-Phenyl-1-[(2*S*)-2-{5-[4-(4-{2-[(2*S*)-1-[(2*R*)-2-phenyl-2-(piperidin-1-yl)acetyl]pyrrolidin-2-yl]-1*H*-imidazol-5-yl}phenyl)phenyl]-1*H*-imidazol-2-yl}pyrrolidin-1-yl]-2-(piperidin-1-yl)ethan-1-one (18). Title compound **18** (free base, white solid). ^{1}H NMR (400 MHz, DMSO-d_6): δ 9.98/9.81 (2 overlapping app br s, ∼2H), 8.07 (app br s, 1.56H), 7.99−7.86 (m, 7.14H), 7.86−7.68 (2 m, 1.17H), 7.68−7.62 (m, 3.16H), 7.62−7.49 (m, 5.67H), 7.45−7.37 (m, 0.40H), 7.26−7.08 (br m, 0.9H), 5.91−5.78 (m, 0.1H), 5.59−5.44 (m overlapped with app s, 2H), 5.32−5.16 (m, 1.9H), 4.12−3.17 (m, 2H), 3.70−3.24 (m, 1.7H), 3.27−2.59 (series of overlapping br m, 6.3H), 2.59−2.30 (m overlapped with DMSO signal, ∼2H), 2.30−2.13 (m, 1.4H), 2.13−1.98 (m, 3.6H), 1.97−1.77 (m, 3.4H), 1.77−1.50 (m, 8.4H), 1.51−1.28 (m, 3.2H). LC (method 10): t_R = 1.85 min. LC/MS (ESI) *m/z*: [M + H]$^+$ calcd for $C_{52}H_{59}N_8O_2$, 827.5; found, 827.2. HRMS (ESI) *m/z*: [M + H]$^+$ calcd for $C_{52}H_{59}N_8O_2$, 827.4761; found, 827.4733.

(2*R*)-2-(Morpholin-4-yl)-1-[(2*S*)-2-{5-[4-(4-{2-[(2*S*)-1-[(2*R*)-2-(morpholin-4-yl)-2-phenylacetyl]pyrrolidin-2-yl]-1*H*-imidazol-5-yl}phenyl)phenyl]-1*H*-imidazol-2-yl}-pyrrolidin-1-yl]-2-phenylethan-1-one (19). Title compound **19** (TFA salt, off-white foam). ^{1}H NMR (400 MHz, DMSO-d_6): δ 8.05 (app br s, 1.84H), 7.99−7.81 (m, 7.63H), 7.77−7.67 (m, 0.61H), 7.67−7.47 (2 m, 8.89H), 7.25−7.10 (m, 1.03H), 5.82−5.77 (m, 0.26H), 5.42 (app br s, 2H), 5.28−5.14 (m, 1.74H), 4.12−3.95 (m, 2.1H), 3.94−3.52 (series of m, 8.1H), 3.52−2.54 (series of overlapping br m, ∼7.8H), 2.50−2.32 (m overlapped with DMSO signal, ∼1.5H), 2.31−2.14 (m, 2.02H), 2.14−1.97 (m, 4H), 1.97−1.83 (m, 2.05H), 1.83−1.66 (m, 0.43H). LC (method 4): t_R = 29.9 min. LC/MS (ESI) *m/z*: [M + H]$^+$ calcd for $C_{50}H_{55}N_8O_4$, 831.43; found, 831.70.

2-[(3*S*)-3-fluoropyrrolidin-1-yl]-1-[(2*S*)-2-{5-[4-(4-{2-[(2*S*)-1-{2-[(3*S*)-3-fluoropyrrolidin-1-yl]-2-phenylacetyl}-pyrrolidin-2-yl]-1*H*-imidazol-5-yl}phenyl)phenyl]-1*H*-imidazol-2-yl}pyrrolidin-1-yl]-2-phenylethan-1-one (20). Title compound **20** (TFA salt, light yellow foam; symmetrical diastereomer-1). ^{1}H NMR (400 MHz, DMSO-d_6): δ 14.57 (s, ∼1H), 10.94 (br s, ∼1H), 8.13 (br s, 2.02H), 8.05−7.87 (m, 7.79H), 7.80−7.64 (m, 4.11H), 7.64−7.53 (m, 5.35H), 7.34−7.25 (m, 0.28H), 7.18−7.11 (m, 0.45H), 5.83−5.70 (m, 0.22H), 5.60/5.50 (2 overlapped app s, 2.95H), 5.37 (app s, 1H), 5.31−5.23 (m, 1.83H), 4.04−2.78 (series of overlapped br m, ∼11H), 2.56−2.35 (br m overlapped with DMSO signal, ∼1H), 2.35−2.11 (m, 4.4H), 2.11−1.78 (m, 7.1H), 1.78−1.57 (m, 0.5H). LC (method 4): t_R = 36.2 min. LC/MS (ESI) *m/z*: [M + H]$^+$ calcd for $C_{50}H_{53}F_2N_8O_2$, 835.4; found, 835.3. HRMS (ESI) *m/z*: [M + H]$^+$ calcd for $C_{50}H_{53}F_2N_8O_2$, 835.4260; found, 835.4261.

2-[(3*S*)-3-fluoropyrrolidin-1-yl]-1-[(2*S*)-2-{5-[4-(4-{2-[(2*S*)-1-{2-[(3*S*)-3-fluoropyrrolidin-1-yl]-2-phenylacetyl}-pyrrolidin-2-yl]-1*H*-imidazol-5-yl}phenyl)phenyl]-1*H*-imidazol-2-yl}pyrrolidin-1-yl]-2-phenylethan-1-one (21). Title compound **21** (TFA salt, off-white foam; symmetrical diastereomer-2). ^{1}H NMR (400 MHz, DMSO-d_6): δ 11.06 (br

s, ∼1H), 8.15−7.79 (series of overlapped m, 10.5H), 7.65−7.55 (m, 3.3H), 7.55−7.48 (m, 3.2H), 7.48−7.38 (m, 3H), 5.59 (app s, 2.14H), 5.53−5.31 (m, 1.34H), 5.28−5.18 (m, 2.07H), 5.07 (app s, 0.23H), 4.94−4.88 (m, 0.22H), 3.99−2.79 (series of overlapping br m, ∼11H), 2.5−1.67 (series of overlapping br m that is partially overlapped with DMSO signal, ∼13H). LC (method 4): t_R = 35.4 min. LC/MS (ESI) *m/z*: $[M + H]^+$ calcd for $C_{50}H_{53}F_2N_8O_2$, 835.4; found, 835.3. HRMS (ESI) *m/z*: $[M + H]^+$ calcd for $C_{50}H_{53}F_2N_8O_2$, 835.4260; found, 835.4266.

(2*R*)-2-(Diethylamino)-2-phenyl-1-[(2*S*)-2-{5-[4-(4-{2-[(2*S*)-1-[(2*R*)-2-phenyl-2-(piperidin-1-yl)acetyl]-pyrrolidin-2-yl]-1*H*-imidazol-5-yl}phenyl)phenyl]-1*H*-imidazol-2-yl}pyrrolidin-1-yl]ethan-1-one (22). Title compound **22** (free base, yellow solid). ^{1}H NMR (400 MHz, DMSO-d_6): δ 11.96 (app br s, 1.6H), 9.79 (app br s, 0.4H), 8.03−7.23 (series of overlapping m, 18.1H), 7.23−6.81 (m, 1.9H), 5.82−5.20 (br m, 1.3H), 5.20−4.99 (m, 1.7H), 4.36−2.25 (series of br m overlapping with each other and that of DMSO signal, ∼11H), 2.23−1.81 (series of m, 8.6H), 1.82−1.27 (series of m, 6.4H), 1.27−0.61 (series of m, 7H). LC (method 11): t_R = 2.53 min. LC/MS (ESI) *m/z*: $[M + H]^+$ calcd for $C_{51}H_{59}N_8O_2$, 815.5; found, 815.2. HRMS (ESI) *m/z*: $[M + H]^+$ calcd for $C_{51}H_{59}N_8O_2$, 815.4761; found, 815.4763.

Methyl *N*-[(1*R*)-2-[(2*S*)-2-{5-[4-(4-{2-[(2*S*)-1-(2-acetamidoacetyl)pyrrolidin-2-yl]-1*H*-imidazol-5-yl}-phenyl)phenyl]-1*H*-imidazol-2-yl}pyrrolidin-1-yl]-2-oxo-1-phenylethyl]carbamate (23). Title compound **23** (TFA salt, off-white foam). ^{1}H NMR (500 MHz, DMSO-d_6): δ 14.43 (br s, ∼2H), 8.16−8.10 (br m, 2H), 8.08−8.00 (m, 1.46H), 8.00−7.93 (m, 3.67H), 7.93−7.86 (m, 3.92H), 7.86−7.75 (series of m, 0.44H), 7.70 (app br d, *J* = 7.9 Hz, 0.69H), 7.44−7.28 (m, 4.39H), 7.05 (app s, 0.43H), 5.71 (app br s, 0.09H), 5.55−5.49 (m, 0.82H), 5.43−5.38 (m, 0.27H), 5.22−5.16 (m, 1.82H), 4.03−3.91 (m, 3H), 3.78−3.72 (m, 1.13H), 3.64−3.57 (m, 1.05H), 3.55/3.53 (2 s, 3H), 3.22−3.14 (m, 0.82H), 2.42−2.23 (2 m, 2.41H), 2.11−2.00 (m, 4.59H), 1.96−1.88 (m, 1H), 1.85/1.81 (2 s, 3H). LC (method 5): t_R = 21.1 min. LC/MS (ESI) *m/z*: $[M + H]^+$ calcd for $C_{40}H_{43}N_8O_5$, 715.3; found, 715.0. HRMS (ESI) *m/z*: $[M + H]^+$ calcd for $C_{40}H_{43}N_8O_5$, 715.3356; found, 715.3369.

Methyl *N*-[(1*R*)-2-[(2*S*)-2-{5-[4-(4-{2-[(2*S*)-1-[(2*R*)-2-acetamidopropanoyl]pyrrolidin-2-yl]-1*H*-imidazol-5-yl}-phenyl)phenyl]-1*H*-imidazol-2-yl}pyrrolidin-1-yl]-2-oxo-1-phenylethyl]carbamate (24). Title compound **24** (TFA salt, off-white solid). ^{1}H NMR (500 MHz, DMSO-d_6): δ 14.32 (br s, ∼3H), 8.31 (app br m, 0.11H), 8.24 (app d, *J* = 6.7 Hz, 0.77H), 8.21−8.03 (m, 1.78H), 8.03−7.88 (m, 7.48H), 7.87−7.64 (series of m, 1.7H), 7.46−7.24 (series of m, 4.62H), 7.05 (app s, 0.54H), 5.89−5.66 (m, 0.24H), 5.57−5.46 (m, 0.79H), 5.40 (app d, *J* = 7.3 Hz, 0.21H), 5.28−5.08 (m, 1.76H), 4.57 (app quint, *J* = 6.9 Hz, 0.82H), 4.31−4.13 (m, 0.18H), 3.99−3.91 (m, 1H), 3.91−3.83 (m, 1H), 3.69−3.58 (m, 1.17H), 3.54/3.53 (2 s, 3H), 3.25−3.12 (m, 0.83H), 2.47−2.33 (m, 1.58H), 2.33−2.15 (m, 1.04H), 2.15−1.96 (m, 4.38H), 1.96−1.88 (m, 1H), 1.87 (s, 2.25H), 1.82/1.81 (2 s, 0.75H), 1.23−1.21 (m, 2.69H), 0.93 (app d, *J* = 6.4 Hz, 0.31H). LC (method 2): t_R = 20.9 min. LC/MS (ESI) *m/z*: $[M + H]^+$ calcd for $C_{41}H_{45}N_8O_5$, 729.4; found, 729.0. HRMS (ESI) *m/z*: $[M + H]^+$ calcd for $C_{41}H_{45}N_8O_5$, 729.3513; found, 729.3530.

Methyl *N*-[(1*R*)-2-[(2*S*)-2-{5-[4-(4-{2-[(2*S*)-1-[(2*S*)-2-acetamidopropanoyl]pyrrolidin-2-yl]-1*H*-imidazol-5-yl}-phenyl)phenyl]-1*H*-imidazol-2-yl}pyrrolidin-1-yl]-2-oxo-1-phenylethyl]carbamate (25). Title compound **25** (TFA salt, off-white foam). ^{1}H NMR (500 MHz, DMSO-d_6): δ 14.48 (br s, ∼3H), 8.33 (app d, *J* = 7.3 Hz, 0.15H), 8.24 (app d, *J* = 7.3 Hz, 0.11H), 8.22−8.08 (m, 2.79H), 8.04−7.88 (m, 7.62H), 7.88−7.65 (m, 1.36H), 7.46−7.23 (m, 4.54H), 7.10−7.00 (m, 0.43H), 5.81−5.71 (m, 0.1H), 5.57−5.48 (m, 0.82H), 5.48−5.37 (m, 0.27H), 5.26−5.11 (m, 1.81H), 4.58 (app quint, *J* = 7.0 Hz, 0.93H), 4.39−4.28 (m, 0.07H), 4.00−3.88 (m, 0.83H), 3.88−3.61 (m, 2.22H), 3.55/3.54/3.53 (3 s, 3H), 3.47−3.34 (m, 0.17H), 3.28−3.10 (m, 0.78H), 2.47−2.34 (m, 1.35H), 2.34−2.19 (m, 0.91H), 2.19−1.84 (2 m, 5.74H), 1.82 (s, 2.64H), 1.69 (s, 0.36H), 1.30−1.19 (m, 3H). LC (method 2): t_R = 20.4 min. LC/MS (ESI) *m/z*: $[M + H]^+$ calcd for $C_{41}H_{45}N_8O_5$, 729.35; found, 729.33.

Methyl *N*-[(1*R*)-2-[(2*S*)-2-{5-[4-(4-{2-[(2*S*)-1-[(2*S*)-2-[(methoxycarbonyl)amino]propanoyl]pyrrolidin-2-yl]-1*H*-imidazol-5-yl}phenyl)phenyl]-1*H*-imidazol-2-yl}-pyrrolidin-1-yl]-2-oxo-1-phenylethyl]carbamate (26). Title compound **26** (TFA salt, off-white foam). ^{1}H NMR (500 MHz, DMSO-d_6): δ 14.44 (br s, ∼3H), 8.21−8.00 (m, 2.07H), 8.00−7.85 (m, 7.65H), 7.85−7.59 (m, 1.35H), 7.45−7.27 (m, 5.26H), 7.05 (app br s, 0.67H), 5.75−5.63 (m, 0.11H), 5.51 (app d, *J* = 7.6 Hz, 0.81H), 5.45−5.31 (m, 0.3H), 5.25−5.09 (m, 1.78H), 4.38 (app quint, *J* = 7.1 Hz, 0.82H), 4.18−4.09 (m, 0.09H), 4.09−4.01 (m, 0.09H), 3.99−3.88 (m, 0.94H), 3.86−3.78 (m, 0.91H), 3.78−3.59 (m, 1.24H), 3.55/3.53 (2 s, 5.7H), 3.37 (s, 0.3H), 3.24−3.12 (m, 0.91H), 2.47−2.32 (m, 1.37H), 2.32−2.16 (m, 1.04H), 2.16−1.97 (m, 4.24H), 1.97−1.73 (m, 1.35H), 1.21 (d, *J* = 6.7 Hz, 3H). LC (method 4): t_R = 26.9 min. LC/MS (ESI) *m/z*: $[M + H]^+$ calcd for $C_{41}H_{45}N_8O_6$, 745.3; found, 745.2. HRMS (ESI) *m/z*: $[M + H]^+$ calcd for $C_{41}H_{45}N_8O_6$, 745.3462; found, 745.3486.

Methyl *N*-[(2*S*)-1-[(2*S*)-2-{5-[4-(4-{2-[(2*S*)-1-[(2*S*)-2-[(methoxycarbonyl)amino]propanoyl]pyrrolidin-2-yl]-1*H*-imidazol-5-yl}phenyl)phenyl]-1*H*-imidazol-2-yl}-pyrrolidin-1-yl]-1-oxopropan-2-yl]carbamate (27). Title compound **27** (TFA salt, light yellow foam). ^{1}H NMR (500 MHz, DMSO-d_6): δ 14.50 (br s, ∼3H), 8.14 (app s, 2H), 7.97 (overlap of d & m, *J* = 8.5 Hz, 4.5H), 7.90 (d, *J* = 8.5 Hz, 3.5H), 7.48−7.44 (m, 1.85H), 7.03 (app br s, 0.15H), 5.42 (app br d, *J* = 8.5 Hz, 0.2H), 5.16 (m, 1.8H), 4.38 (app quint, *J* = 7.1 Hz, 1.8H), 4.11 (app quint, *J* = 7.2 Hz, 0.2H), 3.87−3.78 (m, 1.9H), 3.78−3.66 (m, 2.1H), 3.53 (s, 5.5H), 3.35 (s, 0.5H), 2.45−2.32 (m, 2H), 2.17−1.7 (1 major and 2 minor m, 6H), 1.21 (d, *J* = 7.0 Hz, 6H). LC (method 4): t_R = 20.5 min. LC/MS (ESI) *m/z*: $[M + H]^+$ calcd for $C_{36}H_{43}N_8O_6$, 683.3; found, 682.2. HRMS (ESI) *m/z*: $[M + H]^+$ calcd for $C_{36}H_{43}N_8O_6$, 683.3306; found, 683.3305.

Methyl *N*-[(2*R*)-1-[(2*S*)-2-{5-[4-(4-{2-[(2*S*)-1-[(2*R*)-2-[(methoxycarbonyl)amino]propanoyl]pyrrolidin-2-yl]-1*H*-imidazol-5-yl}phenyl)phenyl]-1*H*-imidazol-2-yl}-pyrrolidin-1-yl]-1-oxopropan-2-yl]carbamate (28). Title compound **28** (TFA salt, white foam). ^{1}H NMR (500 MHz, DMSO-d_6): δ 14.32 (br s, ∼3H), 8.16 (s, 1.77H), 8.07 (app br s, 0.30H), 7.98−7.95 (m, 3.65H), 7.92−7.91 (m, 4.28H), 7.65 (d, *J* = 4.6 Hz, 0.19H), 7.38 (d, *J* = 7.3 Hz, 1.66H), 6.89 (app br s, 0.15H), 5.76 (app br s, 0.2H), 5.17 (m, 1.8H), 4.39 (app quint, *J* = 7.0 Hz, 1.59H), 4.30 (br m, 0.18H), 4.13−4.00 (m, 0.23H), 3.91−3.79 (m, 1.76H), 3.71−3.59 (m, 2.07H), 3.54 (overlapped s & m, 6.17H), 2.46−2.32 (m, 2.21H), 2.23−2.00 (m, 5.29H), 1.97−1.77 (2 m, 0.5H), 1.21 (d, *J* = 7.0 Hz, 5.3H), 0.93 (d, *J* = 6.4 Hz, 0.7H). LC (method 6): t_R = 13.0 min. LC/MS (ESI) *m/z*: $[M + H]^+$ calcd for $C_{36}H_{43}N_8O_6$, 683.3; found,

683.4. HRMS (ESI) m/z: [M + H]$^+$ calcd for $C_{36}H_{43}N_8O_6$, 683.3306; found, 683.3318.

Ethyl *N*-[(2*S*)-1-[(2*S*)-2-{5-[4-(4-{2-[(2*S*)-1-[(2*S*)-2-[(ethoxycarbonyl)amino]propanoyl]pyrrolidin-2-yl]-1*H*-imidazol-5-yl}phenyl)phenyl]-1*H*-imidazol-2-yl}-pyrrolidin-1-yl]-1-oxopropan-2-yl]carbamate (29). Title compound **29** (TFA salt, white foam). ^{1}H NMR (400 MHz, DMSO-d_6): δ 14.48 (br s, ∼3H), 8.13 (s, 2H), 7.98−7.94 (m, 4.3H), 7.89 (d, J = 8.5 Hz, 3.7H), 7.42−7.38 (m, 1.85H), 7.02 (app d, J = 6.0 Hz, 0.15H), 5.40 (app d, J = 8.1 Hz, 0.15H), 5.16 (m, 1.85H), 4.37 (app quint, J = 7.1 Hz, 1.8H), 4.16−4.08 (m, 0.2H), 4.05−3.91 (m, 3.8H), 3.87−3.67 (m, 4.2H), 2.48−2.27 (m, 2.1H), 2.20−2.00 (m, 5.5H), 2.00−1.73 (m, 0.4H), 1.20 (app d, J = 6.8 Hz, 5.84H), 1.15 (app t, J = 7.1 Hz, 5.56H), 0.99 (app t, J = 7.1 Hz, 0.6H). LC (method 6): t_R = 14.2 min. LC/MS (ESI) m/z: [M + H]$^+$ calcd for $C_{38}H_{47}N_8O_6$, 711.4; found, 711.4. HRMS (ESI) m/z: [M + H]$^+$ calcd for $C_{38}H_{47}N_8O_6$, 711.3619; found, 711.3621.

Methyl *N*-{1-[(2*S*)-2-{5-[4-(4-{2-[(2*S*)-1-{2-[(methoxycarbonyl)amino]-2-methylpropanoyl}pyrrolidin-2-yl]-1*H*-imidazol-5-yl}phenyl)phenyl]-1*H*-imidazol-2-yl}-pyrrolidin-1-yl]-2-methyl-1-oxopropan-2-yl}carbamate (30). Title compound **30** (TFA salt, off-white foam). ^{1}H NMR (400 MHz, DMSO-d_6): δ 14.11 (br s, ∼3H), 8.17 (s, 2H), 8.08−7.81 (m, 10H), 5.22 (m, 2H), 3.87−3.69 (m, 3.45H), 3.67 (s, 6H), 3.55−3.38 (m, 0.55H), 2.46−2.23 (m, 2.1H), 2.21−2.05 (m, 2.1H), 2.05−1.87 (m, 3.8H), 1.34 (s, 12H). LC (method 9): t_R = 1.21 min. LC/MS (ESI) m/z: [M + H]$^+$ calcd for $C_{38}H_{47}N_8O_6$, 711.4; found, 711.5. HRMS (ESI) m/z: [M + H]$^+$ calcd for $C_{38}H_{47}N_8O_6$, 711.3619; found, 711.3652.

Methyl *N*-{1-[(2*S*)-2-{5-[4-(4-{2-[(2*S*)-1-{1-[(methoxycarbonyl)amino]cyclopropanecarbonyl}pyrrolidin-2-yl]-1*H*-imidazol-5-yl}phenyl)phenyl]-1*H*-imidazol-2-yl}-pyrrolidine-1-carbonyl]cyclopropyl}carbamate (31). Title compound **31** (TFA salt, off-white solid). ^{1}H NMR (400 MHz, DMSO-d_6): δ 14.36 (br s, ∼3H), 8.21−8.06 (m, 3.33H), 8.02−7.88 (m, 8.03H), 7.82 (app br s, 0.36H), 7.73 (app br s, 0.28H), 5.65 (app br s, 0.23H), 5.21−5.02 (m, 1.77H), 3.97−3.83 (m, 1.6H), 3.83−3.67 (m, 1.86H), 3.62 (s, 4.43H), 3.47 (br s, 1.57H), 3.19 (br s, 0.54H), 2.46−2.27 (m, 1.9H), 2.27−1.81 (m, 5.1H), 1.80−1.43 (m, 1H), 1.38−1.21 (m, 2H), 1.21−1.06 (m, 2H), 1.06−0.90 (m, 2.2H), 0.90−0.65 (m, 1.8H). LC (method 9): t_R = 1.12 min. LC/MS (ESI) m/z: [M + H]$^+$ calcd for $C_{38}H_{43}N_8O_6$, 707.33; found, 707.45. HRMS (ESI) m/z: [M + H]$^+$ calcd for $C_{38}H_{43}N_8O_6$, 707.3306; found, 707.3309.

Methyl *N*-[(2*S*)-1-[(2*S*)-2-{5-[4-(4-{2-[(2*S*)-1-[(2*S*)-2-[(methoxycarbonyl)amino]butanoyl]pyrrolidin-2-yl]-1*H*-imidazol-5-yl}phenyl)phenyl]-1*H*-imidazol-2-yl}-pyrrolidin-1-yl]-1-oxobutan-2-yl]carbamate (32). Title compound **32** (TFA salt, off-white foam). ^{1}H NMR (500 MHz, DMSO-d_6): δ 14.62 (br s, ∼3H), 8.11 (br s, 2H), 8.01−7.92 (m, 4.3H), 7.89 (d, J = 7.9 Hz, 3.7H), 7.42−7.38 (m, 1.87H), 7.04−6.94 (m, 0.13H), 5.48−5.38 (m, 0.15H), 5.15 (dd, J = 7.9, 5.2 Hz, 1.85H), 4.24−4.19 (m, 1.86H), 3.95−3.90 (m, 0.29H), 3.87−3.66 (m, 3.81H), 3.54 (s, 5.34H), 3.45−3.38 (m, 0.26H), 3.36 (s, 0.44H), 2.46−2.30 (m, 2.1H), 2.24−1.98 (m, 5.55H), 1.98−1.90 (m, 0.27H), 1.84−1.63 (m, 2.12H), 1.58−1.35 (m, 1.96H), 0.89−0.84 (m, 6H). LC (method 8): t_R = 1.81 min. LC/MS (ESI) m/z: [M + H]$^+$ calcd for $C_{38}H_{47}N_8O_6$, 711.4; found, 711.4. HRMS (ESI) m/z: [M + H]$^+$ calcd for $C_{38}H_{47}N_8O_6$, 711.3619; found, 711.3643.

Methyl *N*-[(2*S*,3*R*)-3-methoxy-1-[(2*S*)-2-{5-[4-(4-{2-[(2*S*)-1-[(2*S*,3*R*)-3-methoxy-2-[(methoxycarbonyl)amino]butanoyl]pyrrolidin-2-yl]-1*H*-imidazol-5-yl}-phenyl)phenyl]-1*H*-imidazol-2-yl}pyrrolidin-1-yl]-1-oxobutan-2-yl]carbamate (34). Title compound **34** (TFA salt, white solid). ^{1}H NMR (400 MHz, DMSO-d_6): δ 14.66 (br s, ∼3H), 8.14 (br s, 1.88H), 8.04−7.80 (m, 8.12H), 7.27 (d, J = 8.3 Hz, 1.88H), 6.80 (app br s, 0.12H), 5.67 (app d, J = 7.0 Hz, 0.15H), 5.16 (app t, J = 7.0 Hz, 1.85H), 4.33 (dd, J = 8.3, 6.3 Hz, 1.65H), 4.28−4.23 (m, 0.35H), 3.97−3.78 (m, 3.7H), 3.64−3.58 (overlapping m & s, 7H), 3.50−3.40 (m, 0.3H), 3.36 (s, 0.5H), 3.29 (s, 0.5H), 3.21/3.19 (2 overlapping s, 6H), 2.47−2.36 (m, 2.22H), 2.25−1.70 (m, 5.78H), 1.12 (d, J = 6.3 Hz, 0.5H), 1.04 (d, J = 6.3 Hz, 5.5H). LC (method 12): t_R = 2.82 min. LC/MS (ESI) m/z: [M + H]$^+$ calcd for $C_{40}H_{51}N_8O_8$, 771.4; found, 711.2. HRMS (ESI) m/z: [M + H]$^+$ calcd for $C_{40}H_{51}N_8O_8$, 771.3830; found, 771.3802.

Methyl *N*-[(1*S*)-1-cyclopropyl-2-[(2*S*)-2-{5-[4-(4-{2-[(2*S*)-1-[(2*S*)-2-cyclopropyl-2-[(methoxycarbonyl)amino]acetyl]pyrrolidin-2-yl]-1*H*-imidazol-5-yl}phenyl)-phenyl]-1*H*-imidazol-2-yl}pyrrolidin-1-yl]-2-oxoethyl]-carbamate (35). Title compound **35** (TFA salt, off-white foam). ^{1}H NMR (500 MHz, DMSO-d_6): δ 14.59 (br s, ∼3H), 8.12 (br s, 2H), 7.96 (app d, J = 8.2 Hz, 3.7H), 7.90 (app d, J = 8.2 Hz, 4.3H), 7.57 (d, J = 7.9 Hz, 1.69H), 7.44 (app br s, 0.2H), 7.13 (app br s, 0.11H), 5.43 (app br d, J = 7.6 Hz, 0.2H), 5.15 (app dd, J = 7.9, 5.2 Hz, 1.8H), 3.87−3.71 (3 overlapping m, 5.64H), 3.54 (s, 5.35H), 3.49−3.40 (m, 0.36H), 3.33 (s, 0.65H), 2.45−2.30 (m, 2.2H), 2.21−1.72 (series of m, 5.8H), 1.26−1.02 (m, 2H), 0.53−0.35 (m, 5.9H), 0.35−0.28 (m, 1.7H), 0.28−0.19 (m, 0.4H). LC (method 8): t_R = 1.81 min. LC/MS (ESI) m/z: [M + H]$^+$ calcd for $C_{40}H_{47}N_8O_6$, 735.36; found, 735.43. HRMS (ESI) m/z: [M + H]$^+$ calcd for $C_{40}H_{47}N_8O_6$, 735.3619; found, 735.3561.

Methyl *N*-[(2*S*)-1-[(2*S*)-2-{5-[4-(4-{2-[(2*S*)-1-[(2*S*)-2-[(methoxycarbonyl)(methyl)amino]-3-methylbutanoyl]pyrrolidin-2-yl]-1*H*-imidazol-5-yl}phenyl)phenyl]-1*H*-imidazol-2-yl}pyrrolidin-1-yl]-3-methyl-1-oxobutan-2-yl]-*N*-methylcarbamate (36). Title compound **36** (TFA salt, semicrystalline white foam). ^{1}H NMR (400 MHz, DMSO-d_6): δ 14.57 (br s, ∼3H), 8.11 (app br s, 2H), 7.95 (app d, J = 8.1 Hz, 4H), 7.89 (app d, J = 8.1 Hz, 4H), 5.70−5.55 (2 m, 0.2H), 5.24−5.14 (m, 1.8H), 4.61−4.36 (m, 2H), 3.94−3.73 (2 m, 2.3H), 3.69/3.66 (2 s, 5.4H), 3.64−3.42 (2 m, 1.7H), 3.27/3.19 (2 s, 0.6H), 2.72/2.70/2.63/2.60 (4 s, 6H), 2.46−2.32 (m, 2.06H), 2.24−1.93 (m, 7.68H), 1.81−1.64 (m, 0.26H), 0.91−0.88 (m, 0.63H), 0.81−0.77 (m, 10.49H), 0.74−0.59 (2 m, 0.88H). LC (method 9): t_R = 1.46 min. LC/MS (ESI) m/z: [M + H]$^+$ calcd for $C_{42}H_{55}N_8O_6$, 767.4; found, 767.4. HRMS (ESI) m/z: [M + H]$^+$ calcd for $C_{42}H_{55}N_8O_6$, 767.4245; found, 767.4252.

***N*-[(2*S*)-1-[(2*S*)-2-{5-[4-(4-{2-[(2*S*)-1-[(2*S*)-2-acetamido-3-methylbutanoyl]pyrrolidin-2-yl]-1*H*-imidazol-5-yl}-phenyl)phenyl]-1*H*-imidazol-2-yl}pyrrolidin-1-yl]-3-methyl-1-oxobutan-2-yl]acetamide (37).** Title compound **37** (TFA salt, white solid). ^{1}H NMR (500 MHz, DMSO-d_6): δ 14.63 (br s, ∼3H), 8.23−8.09 (m, 2.16H), 8.04 (d, J = 8.5 Hz, 1.92H), 8.01−7.92 (m, 4.39H), 7.90 (app d, J = 8.5 Hz, 3.53H), 5.60 (app d, J = 7.3 Hz, 0.23H), 5.14 (app t, J = 7.2 Hz, 1.77H), 4.38 (app t, J = 7.9 Hz, 1.75H), 4.19 (app t, J = 7.9 Hz, 0.25H), 3.97−3.87 (m, 1.73H), 3.87−3.77 (m, 1.78H), 3.76−3.63 (m, 0.28H), 3.54−3.38 (m, 0.21H), 2.49−2.24 (m, 2.42H), 2.23−1.91 (m, 7.58H), 1.87 (s, 5.41H), 1.74 (s, 0.59H), 0.97−0.88

(m, 1.15H), 0.83 (d, J = 6.7 Hz, 5.25H), 0.80 (d, J = 6.7 Hz, 5.60H). LC (method 13): t_R = 2.05 min. LC/MS (ESI) m/z: [M + H]$^+$ calcd for $C_{40}H_{51}N_8O_4$, 707.40; found, 707.77. HRMS (ESI) m/z: [M + H]$^+$ calcd for $C_{40}H_{51}N_8O_4$, 707.4033; found, 707.4004.

***N*-[(2*R*)-1-[(2*S*)-2-{5-[4-(4-{2-[(2*S*)-1-[(2*R*)-2-acetamido-3-methylbutanoyl]pyrrolidin-2-yl]-1*H*-imidazol-5-yl}-phenyl)phenyl]-1*H*-imidazol-2-yl}pyrrolidin-1-yl]-3-methyl-1-oxobutan-2-yl]acetamide (38).** Title compound **38** (TFA salt, off-white solid). ^{1}H NMR (500 MHz, DMSO-d_6): δ 14.33 (br s, ∼3H), 8.30 (br d, J = 6.7 Hz, 0.33H), 8.21−8.03 (m, 3.79H), 8.03−7.79 (m, 7.88H), 6.08−5.88 (m, 0.25H), 5.23 (dd, J = 8.2, 4.0 Hz, 1.75H), 4.43 (app t, J = 7.8 Hz, 1.64H), 3.99−3.87 (m, 2.28H), 3.76−3.62 (m, 1.86H), 3.52−3.40 (m, 0.22H), 2.48−2.26 (m, 2.03H), 2.20−2.00 (m, 5.33H), 2.00−1.91 (m, 2.29H), 1.90 (s, 5.11H), 1.87 (s, 0.89H), 1.84−1.75 (m, 0.35H), 0.97−0.84 (m, 10.44H), 0.73 (d, J = 6.7 Hz, 0.81H), 0.45 (d, J = 6.4 Hz, 0.75H). LC (method 8): t_R = 1.93 min. LC/MS (ESI) m/z: [M + H]$^+$ calcd for $C_{40}H_{51}N_8O_4$, 707.4; found, 707.6. HRMS (ESI) m/z: [M + H]$^+$ calcd for $C_{40}H_{51}N_8O_4$, 707.4033; found, 707.4054.

Methyl *N*-[(2*S*)-1-[(2*S*)-2-{5-[4-(4-{2-[(2*S*)-1-[(2*R*)-2-(diethylamino)-2-phenylacetyl]pyrrolidin-2-yl]-1*H*-imidazol-5-yl}phenyl)phenyl]-1*H*-imidazol-2-yl}pyrrolidin-1-yl]-1-oxopropan-2-yl]carbamate (39). Title compound **39** (TFA salt, white foam). ^{1}H NMR (500 MHz, DMSO-d_6): δ 14.61 (br s, ∼2H), 9.82 (br s, ∼1H), 8.13 (s, 1.26H), 8.06 (br s, 0.9H), 8.00−7.85 (m, 7.89H), 7.81−7.64 (m, 2.04H), 7.63−7.51 (m, 2.68H), 7.49−7.42 (m, 0.77H), 7.23 (m, 0.18H), 7.16 (m, 0.26H), 7.03 (m, 0.02H), 5.99 (app br s, 0.1H), 5.55 (app br s, 0.16H), 5.44 (s, 0.96H), 5.24−5.10 (m, 1.78H), 4.44−4.31 (m, 0.93H), 4.16−4.04 (m, 1H), 3.88−3.70 (2 m, 2.07H), 3.53 (s, 2.73H), 3.35 (s, 0.27H), 3.34−3.12 (m, 2H), 3.12−3.01 (m, 1H), 2.98−2.84 (app br s, 1H), 2.65−2.53 (br m partially overlapped with DMSO signal, 1H), 2.47−2.30 (m, 1.16H), 2.30−2.16 (m, 0.94H), 2.16−1.98 (m, 4.5H), 1.98−1.66 (m, 1.4H), 1.34−1.00 (d overlapped with series of m, J = 7.0 Hz, 9H). LC (method 6): t_R = 12.60 min. LC/MS (ESI) m/z: [M + H]$^+$ calcd for $C_{43}H_{51}N_8O_4$, 743.4; found, 743.5. HRMS (ESI) m/z: [M + H]$^+$ calcd for $C_{43}H_{51}N_8O_4$: 743.4033; found, 743.4053.

Methyl *N*-[(2*S*)-1-[(2*S*)-2-{5-[4-(4-{2-[(2*S*)-1-[(2*R*)-2-(diethylamino)-2-phenylacetyl]pyrrolidin-2-yl]-1*H*-imidazol-5-yl}phenyl)phenyl]-1*H*-imidazol-2-yl}pyrrolidin-1-yl]-1-oxobutan-2-yl]carbamate (40). Title compound **40** (TFA salt, light-yellow foam). ^{1}H NMR (500 MHz, DMSO-d_6): δ 14.71 (br s, ∼3H), 9.78 (br s, ∼1H), 8.13 (app br s, 1.26H), 8.04 (app br s, 0.97H), 7.99−7.82 (m, 7.80H), 7.78−7.64 (m, 2H), 7.63−7.51 (m, 2.67H), 7.44 (app d, J = 8.5 Hz, 0.09H), 7.39 (d, J = 7.9 Hz, 0.75H), 7.29−7.19 (m, 0.19H), 7.19−7.09 (m, 0.24H), 7.03−6.92 (m, 0.03H), 5.98 (app br s, 0.09H), 5.54 (app br s, 0.13H), 5.49−5.40 (m, 0.98H), 5.25−5.08 (m, 1.8H), 4.28−4.16 (m, 0.97H), 4.16−4.04 (m, 0.93H), 3.91−3.64 (m, 2.16H), 3.54 (s, 2.76H), 3.35 (s, 0.24H), 3.33−3.13 (m, 1.8H), 3.13−2.99 (m, 1.11H), 2.99−2.80 (m, 1.03H), 2.68−2.51 (m, ∼1H), 2.45−2.32 (m, 1.44H), 2.28−1.86 (series of m, 6.56H), 1.82−1.68 (m, 1H), 1.53−1.42 (m, 1H), 1.34−0.98 (series of m, 5.97H), 0.90−0.84 (m, 3.03H). LC (method 8): t_R = 1.74 min. LC/MS (ESI) m/z: [M + H]$^+$ calcd for $C_{44}H_{53}N_8O_4$, 757.4; found, 757.4. HRMS (ESI) m/z: [M + H]$^+$ calcd for $C_{44}H_{53}N_8O_4$, 757.4190; found, 757.4212.

Methyl *N*-[(2*S*)-1-[(2*S*)-2-{5-[4-(4-{2-[(2*S*)-1-[(2*R*)-2-(diethylamino)-2-phenylacetyl]pyrrolidin-2-yl]-1*H*-imidazol-5-yl}phenyl)phenyl]-1*H*-imidazol-2-yl}pyrrolidin-1-yl]-3-methyl-1-oxobutan-2-yl]carbamate (41). Title compound **41** (TFA salt, tan foam). ^{1}H NMR (500 MHz, DMSO-d_6): δ 14.74 (br s, ∼2H), 9.80 (br s, ∼1H), 8.12 (app br s, 1.24H), 8.09−7.82 (m, 8.71H), 7.82−7.65 (m, 2.05H), 7.65−7.42 (m, 2.80H), 7.33 (d, J = 8.5 Hz, 0.79H), 7.27−7.19 (m, 0.20H), 7.18−7.12 (m, 0.21H), 5.96 (app br s, 0.09H), 5.64−5.49 (m, 0.24H), 5.44 (app s, 0.87H), 5.25−5.06 (m, 1.8H), 4.21−4.03 (m, 1.80H), 3.95−3.68 (m, 2.20H), 3.54 (s, 2.75H), 3.34 (s, 0.25H), 3.33−3.13 (m, 2H), 3.13−3.02 (m, 1H), 3.02−2.79 (m, 1H), 2.68−2.54 (m, ∼1H), 2.46−2.30 (m, 1.3H), 2.30−2.14 (m, 1.79H), 2.14−1.96 (m, 4.76H), 1.96−1.84 (m, 0.98H), 1.84−1.63 (m, 0.17H), 1.38−0.96 (series of m, 6H), 0.96−0.85 (m, 1.18H), 0.84 (d, J = 6.7 Hz, 2.32H), 0.79 (d, J = 6.7 Hz, 2.50H). LC (method 8): t_R = 1.76 min. LC/MS (ESI) m/z: [M + H]$^+$ calcd for $C_{45}H_{55}N_8O_4$, 771.4; found, 771.5. HRMS (ESI) m/z: [M + H]$^+$ calcd for $C_{45}H_{55}N_8O_4$, 771.4346; found, 771.4379.

Virology Assay. The tabulated activity and cytotoxicity data are mean values of at least two experiments, and in general, the replicon assay exhibits a maximum of 3-fold variation. GT-1a/-1b HCV and BVDV EC_{50} values were obtained from FRET and Luciferase assays, respectively. Details of the biological assays used in the characterizations of final compounds are provided in ref 6d.

PK Assessment. Rat PK studies (4 and/or 24 h): Two animals per dosing group were used in the 4 h rat PK screens, where plasma was sampled at 0.25, 0.5, 1, 2, and 4 h, and liver samples were obtained at the 4 h study termination. In the case of 24 h rat PK studies, a total of three animals per dosing group were used, where plasma was sampled for a total of eight time points (0.25, 0.5, 1, 2, 4, 6, 8, and 24 h), and liver samples were obtained at study termination. Unless noted otherwise, PEG-400 was the dosing vehicle for the rat PK studies.

Vehicle information for multispecies PO-PK data summarized in Table 8: compound **33**, rat (100% PEG-400); dog (60% PEG-400, 10% ethanol, 30% water); monkey (PEG-400/povidone K-30/Vitamin E TPGS/Tween-80 in 95:2:2:1 ratio). Compound **39**, rat, dog, and monkey (PEG-400/povidone K-30/Vitamin E TPGS/Tween-80 in 95:2:2:1 ratio).

Bioactivation Study. The compound (10 μM) was incubated with human liver microsomes (1 mg protein/mL) in phosphate buffer (50 mM; pH 7.4) at 37 °C for 30 min. The incubation was supplemented with NADPH (1 mM) and either GSH (5 mM) or potassium cyanide (1 mM). The incubation mixture was treated with a single volume of CH_3CN and centrifuged at 1000g to obtain supernatant, which was stored at 4 °C until LC/MS analysis. Chromatographic separation was carried out using an HPLC system that consisted of a Waters (Milford, MA) Alliance 2695 Separations Module and a Phenomenex Luna C18 column (2 × 150 mm, 3 μm). The mobile phase consisted of 10 mM NH_4OAc (pH 5) in H_2O/CH_3CN (95/5 v/v) (solvent-A) and CH_3CN (solvent-B) at 200 μL/min with the following gradient conditions: 0% B isocratic for 5 min, 0−90% B over 25 min, and 90% B isocratic for 15 min. Assessment for the presence of GSH and cyano adducts was made on the basis of LC/MS and LC/MS/MS data.

Solubility Assessment. The compound is incubated in 25 mM aqueous phosphate buffer (pH 6.5) in a sealed 1 fluid dram glass vial at 22 °C for 24 h, while being agitated with an

Orbitron Rotator. The mixture was centrifuged and filtered through a 0.45 μm PTFE filter membrane. To minimize a potential filter-adsorption effect, the first 100 μL of the filtrate was discarded. Sample concentration was determined by HPLC using an Agilent 1200 equipped with UV detection.

AUTHOR INFORMATION

Corresponding Author

*E-mail: makonen.belema@bms.com. Tel.: 1-203-677-6928.

Notes

The authors declare no competing financial interest.

The discovery chemistry effort at Bristol-Myers Squibb Pharmaceutical Research Institute, Candiac, Que. lasted until June 2007.

ACKNOWLEDGMENTS

We thank the following members of our analytical and separation groups for the diverse role they played in enabling the work described in this manuscript: Jingfang Cutrone, Dieter Drexler, Xiaohu Huang, Edward S. Kozlowski, and Julia M. Nielson. We thank Gerry G. Everlof and Lucy Sun for conducting the solubility and the patch-clamp ion channel inhibition assessments, respectively, and John G. Houston and Carl P. Decicco for their guidance and support.

REFERENCES

(1) (a) Vaidya, A.; Perry, C. M. Simeprevir: First global approval. *Drugs* **2013**, *73*, 2093−2106, and references cited therein. (b) Lawitz, E.; Mangia, A.; Wyles, D.; Rodriguez-Torres, M.; Hassanein, T.; Gordon, S. C.; Schultz, M.; Davis, M. N.; Kayali, Z.; Reddy, K. R.; Jacobson, I. M.; Kowdley, K. V.; Nyberg, L.; Subramanian, G. M.; Hyland, R. H.; Arterburn, S.; Jiang, D.; McNally, J.; Brainard, D.; Symonds, W. T.; McHutchison, J. G.; Sheikh, A. M.; Younossi, Z.; Gane, E. J. Sofosbuvir for previously untreated chronic hepatitis C infection. *N. Engl. J. Med.* **2013**, *368*, 1878−1887. (c) Gilead Sciences, Inc. U.S. Food and Drug Administration approves Gilead's Sovaldi™ (sofosbuvir) for the treatment of chronic hepatitis C. http://www.gilead.com/news/press-releases, Dec. 6, 2013.

(2) Gao, M.; Nettles, R. E.; Belema, M.; Snyder, L. B.; Nguyen, V. N.; Fridell, R. A.; Serrano-Wu, M. H.; Langley, D. R.; Sun, J.-H.; O'Boyle, D. R., II; Lemm, J. A.; Wang, C.; Knipe, J. O.; Chien, C.; Colonno, R. J.; Grasela, D. M.; Meanwell, N. A.; Hamann, L. G. Chemical genetics strategy identifies an HCV NS5A inhibitor with a potent clinical effect. *Nature* **2010**, *465*, 96−100.

(3) (a) Link, J. O.; Taylor, J. G.; Xu, L.; Mitchell, M. L.; Guo, H.; Liu, H.; Kato, D.; Kirschberg, T.; Sun, J.; Squires, N.; Parrish, J.; Kellar, T.; Yang, Z.-Y.; Yang, C.; Matles, M.; Wang, Y.; Wang, K.; Cheng, G.; Tian, Y.; Mogalian, E.; Mondou, E.; Cornpropst, M.; Perry, J.; Desai, M. C. The discovery of ledipasvir (GS-5885), a potent once-daily oral NS5A inhibitor for the treatment of hepatitis C virus infection. *J. Med. Chem.* DOI: 10.1021/jm401499. (b) Wilfret, D. A.; Walker, J.; Adkison, K. K.; Jones, L. A.; Lou, Y.; Gan, J.; Castellino, S.; Moseley, C. L.; Horton, J.; de Serres, M.; Culp, A.; Goljer, I.; Spreen, W. Safety, tolerability, pharmacokinetics, and antiviral activity of GSK2336805, an inhibitor of hepatitis C virus NS5A, in healthy subjects and subjects chronically infected with genotype 1 hepatitis C virus. *Antimicrob. Agents Chemother.* **2013**, *57*, 5037−5044. (c) Coburn, C. A.; Meinke, P. T.; Chang, W.; Fandozzi, C. M.; Graham, D. J.; Hu, B.; Huang, Q.; Kargman, S.; Kozlowski, J.; Liu, R.; McCauley, J. A.; Nomeir, A. A.; Soll, R. M.; Vacca, J. P.; Wang, D.; Wu, H.; Zhong, B.; Olsen, D. B.; Ludmerer, S. W. Discovery of MK-8742: An HCV NS5A inhibitor with broad genotype activity. *ChemMedChem* **2013**, *8*, 1930−1940.

(4) (a) O'Boyle, D. R., II; Nower, P. T.; Lemm, J. A.; Valera, L.; Sun, J.-H.; Rigat, K.; Colonno, R.; Gao, M. Development of a cell-based high-throughput specificity screen using a hepatitis C virus-bovine viral diarrhea virus dual replicon assay. *Antimicrob. Agents Chemother.* **2005**, *49*, 1346−1353. (b) Lemm, J. A.; O'Boyle, D. R., II; Liu, M.; Nower, P. T.; Colonno, R.; Deshpande, M. S.; Snyder, L. B.; Martin, S. W.; St. Laurent, D. R.; Serrano-Wu, M. H.; Romine, J. L.; Meanwell, N. A.; Gao, M. Identification of hepatitis C virus NS5A inhibitors. *J. Virol.* **2010**, *84*, 482−491. (c) Lemm, J. A.; Leet, J. E.; O'Boyle, D. R., II; Romine, J. L.; Huang, X. S.; Schroeder, D. R.; Alberts, J.; Cantone, J. L.; Sun, J.-H.; Nower, P. T.; Martin, S. W.; Serrano-Wu, M. H.; Meanwell, N. A.; Snyder, L. B.; Gao, M. Discovery of potent hepatitis C virus NS5A inhibitors with dimeric structures. *Antimicrob. Agents Chemother.* **2011**, *55*, 3795−3802.

(5) For additional chemotypes that emerged from screening efforts and were reported to target the NS5A protein based on resistance mapping, see: (a) Najarro, P.; Mathews, N.; Cockerill, S. NS5A inhibitors. *Hepatitis C Viruses*, Tan, S. -L., Ed.; Horizon Bioscience: Wymondham, U.K, 2006; pp 271−292. (b) Conte, I.; Giuliano, C.; Ercolani, C.; Narjes, F.; Koch, U.; Rowley, M.; Altamura, S.; De Francesco, R.; Neddermann, P.; Migliaccio, G.; Stansfield, I. Synthesis and SAR of piperazinyl-*N*-phenylbenzamides as inhibitors of hepatitis C virus RNA replication in cell culture. *Bioorg. Med. Chem. Lett.* **2009**, *19*, 1779−1783. (c) Krueger, A. C.; Madigan, D. L.; Beno, D. W.; Betebenner, D. A.; Carrick, R.; Green, B. E.; He, W.; Liu, D.; Maring, C. J.; McDaniel, K. F.; Mo, H.; Molla, A.; Motter, C. E.; Pilot-Matias, T. J.; Tufano, M. D.; Kempf, D. J. Novel hepatitis C virus replicon inhibitors: synthesis and structure−activity relationships of fused pyrimidine derivatives. *Bioorg. Med. Chem. Lett.* **2012**, *22*, 2212−2215. (d) DeGoey, D. A.; Betebenner, D. A; Grampovnik, D. J.; Liu, D.; Pratt, J. K.; Tufano, M. D.; He, W.; Krishnan, P.; Pilot-Matias, T. J.; Marsh, K. C.; Molla, A.; Kempf, D. J.; Maring, C. J. Discovery of pyrido[2,3-*d*]pyrimidine-based inhibitors of HCV NS5A. *Bioorg. Med. Chem. Lett.* **2013**, *23*, 3627−3630.

(6) (a) Romine, J. L.; St. Laurent, D. R.; Leet, J. E.; Martin, S. W.; Serrano-Wu, M. H.; Yang, F.; Gao, M.; O'Boyle, D. R., II; Lemm, J. A.; Sun, J.-H.; Nower, P. T.; Huang, X.; Deshpande, M. S.; Meanwell, N. A.; Snyder, L. B. Inhibitors of HCV NS5A: From iminothiazolidinones to symmetrical stilbenes. *ACS Med. Chem. Lett* **2011**, *2*, 224−229. (b) St. Laurent, D. R.; Belema, M.; Gao, M.; Goodrich, J.; Kakarla, R.; Knipe, J. O.; Lemm, J. A.; Liu, M.; Lopez, O. D.; Nguyen, V. N.; Nower, P. T.; O'Boyle, D., II; Qiu, Y.; Romine, J. L.; Serrano-Wu, M. H.; Sun, J.-H.; Valera, L.; Yang, F.; Yang, X.; Meanwell, N. A.; Snyder, L. B. HCV NS5A replication complex inhibitors. Part 2: Investigation of stilbene prolinamides. *Bioorg. Med. Chem. Lett.* **2012**, *22*, 6063−6066. (c) Lopez, O. D.; Nguyen, V. N.; St. Laurent, D. R.; Belema, M.; Serrano-Wu, M. H.; Goodrich, J. T.; Yang, F.; Qiu, Y.; Ripka, A. S.; Nower, P. T.; Valera, L.; Liu, M.; O'Boyle, D. R., II; Sun, J.-H.; Fridell, R. A.; Lemm, J. A.; Gao, M.; Good, A. C.; Meanwell, N. A.; Snyder, L. B. HCV NS5A replication complex inhibitors. Part 3: Discovery of potent analogues with distinct core topologies. *Bioorg. Med. Chem. Lett.* **2013**, *23*, 779−784. (d) St. Laurent, D. R.; Serrano-Wu, M. H.; Belema, M.; Ding, M.; Fang, H.; Gao, M.; Goodrich, J. T.; Krause, R. G.; Lemm, J. A.; Liu, M.; Lopez, O.; Nguyen, V. N.; Nower, P. T.; O'Boyle, D. R., II; Pearce, B. C.; Romine, J. L.; Valera, L.; Sun, J.-H.; Wang, Y.-K.; Yang, F.; Yang, X.; Meanwell, N. A.; Snyder, L. B. HCV NS5A replication complex inhibitors. Part 4: Optimization for genotype 1a replicon inhibitory activity. *J. Med. Chem.* DOI: 10.1021/jm301796k. (e) Belema, M.; Nguyen, V. N.; St. Laurent, D. R.; Lopez, O. D.; Qiu, Y.; Good, A. C.; Nower, P. T.; Valera, L.; O'Boyle, D. R., II; Sun, J.-H.; Liu, M.; Fridell, R. A.; Lemm, J. A.; Gao, M.; Knipe, J. O.; Meanwell, N. A.; Snyder, L. B. HCV NS5A replication complex inhibitors. Part 5: Discovery of potent and pan-genotypic glycinamide cap derivatives. *Bioorg. Med. Chem. Lett.* **2013**, *23*, 4428−4435. (f) Belema, M.; Nguyen, V. N.; Romine, J. L.; St. Laurent, D. R.; Lopez, O. D.; Goodrich, J.; Nower, P. T.; O'Boyle, D. R., II; Lemm, J. A.; Fridell, R. A.; Gao, M.; Fang, H.; Krause, R. G.; Wang, Y.-K.; Oliver, A. J.; Good, A. C.; Knipe, J. O.; Meanwell, N. A.; Snyder, L. B. Hepatitis C virus NS5A replication complex inhibitors. Part 6: The discovery of a novel and highly potent biarylimidazole chemotype with inhibitory activity toward genotypes 1a and 1b replicons. *J. Med. Chem.* DOI:10.1021/jm4016203.

(7) For details on the PK studies, see the general Experimental Section.
(8) *Bis*-(*S*)-phenylglycine diastereomer of **2**: GT-1a/-1b EC_{50} = 1.6 nM/0.046 nM; both GT-1b CC_{50} and BVDV EC_{50} values were >10 μM.
(9) Lovering, F.; Bikker, J.; Humblet, C. Escape from flatland: Increasing saturation as an approach to improving clinical success. *J. Med. Chem.* **2009**, *52*, 6752−6756. (b) Ritchie, T. J.; Macdonald, S. J. F. The impact of aromatic ring count on compound developability—are too many aromatic rings a liability in drug design? *Drug Discovery Today* **2009**, *14*, 1011−1020.
(10) Wang, C.; Valera, L.; Jia, L.; Kirk, M. J.; Gao, M.; Fridell, R. A. In vitro activity of daclatasvir on hepatitis C virus genotype 3 NS5A. *Antimicrob. Agents Chemother.* **2013**, *57*, 611−613.
(11) A manuscript detailing the ADME characterization of **33** is in preparation and will be published elsewhere.
(12) Nettles, R. E.; Gao, M.; Bifano, M.; Chung, E.; Persson, A.; Marbury, T. C.; Goldwater, R.; DeMicco, M. P.; Rodriguez-Torres, M.; Vutikullird, A.; Fuentes, E.; Lawitz, E.; Lopez-Talavera, J. C.; Grasela, D. M. Multiple ascending dose study of BMS-790052, a nonstructural protein 5A replication complex inhibitor, in patients infected with hepatitic C virus genotype 1. *Hepatology* **2011**, *54*, 1956−1965.
(13) (a) Lok, A. S.; Gardiner, D. F.; Lawitz, E.; Martorell, C.; Everson, G. T.; Ghalib, R.; Reindollar, R.; Rustgi, V.; McPhee, F.; Wind-Rotolo, M.; Persson, A.; Zhu, K.; Dimitrova, D. I.; Eley, T.; Guo, T.; Grasela, D. M.; Pasquinelli, C. Preliminary study of two antiviral agents for hepatitis C genotype 1. *N. Engl. J. Med.* **2012**, *366*, 216−224. (b) Chayanna, K.; Takahashi, S.; Toyota, J.; Karino, Y.; Ikeda, K.; Ishikawa, H.; Watanabe, H.; McPhee, F.; Hughes, E.; Kumada, H. Dual therapy with the nonstructural protein 5A inhibitor, daclatasvir, and the nonstructural protein 3 protease inhibitor, asunaprevir, in hepatitis C virus genotype 1b-infected null responders. *Hepatology* **2012**, *55*, 742−748. (c) Suzuki, Y.; Ikeda, K.; Suzuki, F.; Toyota, J.; Karino, Y.; Chayama, K.; Kawakami, Y.; Ishikawa, H.; Watanabe, H.; Hu, W.; Eley, T.; McPhee, F.; Hughes, E.; Kumada, H. Dual oral therapy with daclatasvir and asunaprevir for patients with HCV genotype 1b infection and limited treatment options. *J. Hepatology* **2013**, *58*, 655−662. (d) Pol, S.; Ghalib, R. H.; Rustgi, V. K.; Matorell, C.; Everson, G. T.; Tatum, H. A.; Hezode, C.; Lim, J. K.; Bronowicki, J. P.; Abrams, G. A.; Brau, N.; Morris, D. W.; Thuluvath, P. J.; Reindollar, R. W.; Yin, P. D.; Diva, U.; Hindes, R.; McPhee, F.; Hernandez, D.; Wind-Rotolo, M.; Hughes, E. A.; Schnittman, S. Daclatasvir for previously untreated chronic hepatitis C genotype-1 infection: a randomized, parallel-group, double-blind, placebo-controlled, dose-finding phase 2a trial. *Lancet* **2012**, *12*, 671−677.
(14) Herbst, D. A.; Reddy, K. R. NS5A inhibitor, daclatasvir, for the treatment of chronic hepatitis C virus infection. *Expert Opin. Invest. Drugs* **2013**, *22*, 1337−1346.
(15) Everson, G. T.; Sims, K. D.; Rodriguez-Torres, M.; Hezode, C.; Lawitz, E.; Bourliere, M.; Loustaud-Ratti, V.; Rustgi, V.; Schwartz, H.; Tatum, H.; Marcellin, P.; Pol, S.; Thuluvath, P. J.; Eley, T.; Wang, X.; Huang, S.-P.; McPhee F.; Wind-Rotolo, M.; Chung, E.; Pasquinelli C.; Grasela, D. M.; Gardiner, D. F. Efficacy of an interferon- and Ribavirin-free regimen of daclatasvir, asunaprevir, and BMS-791325 in treatment-naïve patients with HCV genotype 1 infection. *Gastroenterology* **2014**, *146*, 420−429.
(16) (a) Targett-Adams, P.; Graham, E. J. S.; Middleton, J.; Palmer, A.; Shaw, S. M.; Lavender, H.; Brain, P.; Tran, T. D.; Jones, L. H.; Wakenhut, F.; Stammen, B.; Pryde, D.; Pickford, C.; Westby, M. Small molecules targeting hepatitis C virus-encoded NS5A cause subcellular redistribution of their target: Insights into compound modes of action. *J. Virol.* **2011**, *85*, 6353−6368. (b) Lee, C.; Ma, H.; Hang, J. Q.; Leveque, V.; Sklan, E. H.; Elazar, M.; Klumpp, K.; Glenn, J. S. The hepatitis C virus NS5A inhibitor (BMS-790052) alters the subcellular localization of the NS5A non-structural viral protein. *Virology* **2011**, *414*, 10−18. (c) Guedj, J.; Dahari, H.; Rong, L.; Sansone, N. D.; Nettles, R. E.; Cotler, S. J.; Layden, T. J.; Uprichard, S. L.; Perelson, A. S. Modeling shows that the NS5A inhibitor daclatasvir has two modes of action and yields a shorter estimate of the hepatitis C virus half-life. *Proc. Natl. Acad. Sci. U.S.A.* **2013**, *110*, 3991−3996.
(17) Bachand, C.; Belema, M.; Deon, D. H.; Good, A. C.; Goodrich, J. T.; James, C. A.; Lavoie, R.; Lopez, O. D.; Martel, A.; Meanwell, N. A.; Nguyen, V. N.; Romine, J. L.; Ruediger, E. H.; Snyder, L. B.; St. Laurent, D. R.; Yang, F.; Langley, D. R.; Wang, G.; Hamann, L. G. Hepatitis C Virus Inhibitors. PCT Intl. Application. 2008, Patent No. WO2008-021927.
(18) Poitout, L.; Roubert, P.; Contour-Galcera, M.-O.; Moinet, C.; Lannoy, J.; Pommier, J.; Plas, P.; Bigg, D.; Thurieau, C. Identification of potent non-peptide somatostatin antagonists with sst3 selectivity. *J. Med. Chem.* **2001**, *44*, 2990−3000.
(19) Wang, X.; Rabbat, P.; O'Shea, P.; Tillyer, R.; Grabowski, E. J. J.; Reider, P. J. Selective monolithiation of 2,5-dibromopyridine with butyllithium. *Tetrahedon Lett* **2000**, *41*, 4335−4338.
(20) Shah, N.; Pierce, T.; Kowdley, K. V. Review of direct-acting antiviral agents for the treatment of chronic hepatitis C. *Expert Opin. Invest. Drugs* **2013**, *22*, 1107−1121.
(21) The generic description of the Experimental Section is a slightly modified version of a paragraph provided in ref 6f for a related work disclosed by the same authors.

■ NOTE ADDED AFTER ASAP PUBLICATION

After this paper was published ASAP on February 12, 2014, text changes were made in last two paragraphs of the Results and Discussion section. The corrected version was reposted March 13, 2014.